Evaluation of a Pneumatic Cylinder for Actuation of an Ankle Exoskeleton

by

David S. Bell

A thesis submitted to the Graduate Faculty of
Auburn University
in partial fulfillment of the
requirements for the Degree of
Master of Science

Auburn, Alabama
December 9, 2023

Keywords; Controls, Exoskeleton, Pneumatics, Robotics, Actuation

Approved by

Dr. Micheal Zabala, Chair, Associate Professor of Mechanical Engineering
Dr. Chad Rose, Assistant Professor of Mechanical Engineering
Dr. Brendon Allen, Assistant Professor of Mechanical Engineering

Abstract

Ankle exoskeletons are used to reduce the effort of walking. This research aims to design and test an actuator that takes advantage of new joint angle prediction methods. First, a Maxon EC motor was tested on an exoskeleton emulator using a position and velocity cascaded controller to follow a recorded ankle angle profile. It performed well and met requirements but also showed shortcomings in speed, safety, and fault tolerance. A study was done on alternative actuation technologies resulting in pneumatics being selected for prototyping. A pneumatic cylinder has advantages in this application such as speed, force to weight, and compliance to the wearer. For this study servo valves were used to control a prototype pneumatic actuator. The prototype actuator system was tested using data from human motion capture for velocity profile movement control and derivative based force output control in fixed and loaded cases. We evaluated the performance of the controllers for stability, movement speed, force, response delay, and accuracy based on delayed percent RMSE. The design met performance goals but was not as accurate as expected due to the lack of direct position feedback control needed to maintain stability at high speeds. The controller tracked the velocity profile of the test subjects but with a large position bias. Force control using ankle moment data was also highly inaccurate. Overall, this system shows promise for applications with simpler control needs or lower actuation speeds with high force.

Acknowledgments

Thanks to Dr. Zabala for providing interesting research and mentoring me in writing and becoming a better researcher. I would also like to thank Dr. Rose and Dr. Allen for their advice on controllers and for being on my committee. Thanks to the other students in the AUBE lab, David Hollinger, Sarah, Sierra, Jaxxie, Markham, Ryan, and Ethan for collaboration, moral support, and being fun to work around. Former GAVLAB members Sam Douglass, Howard Chen, Archit, Ryan McWilliams and Stephanie also provided advice and encouragement.

I never expected to complete this degree until Dr. Zabala invited me to restart the program in the AUBE lab. My family, friends and the community at Grace Auburn Church helped and encouraged me through some difficult times in life and made this possible. Thanks to my parents and grandparents for helping me financially for way longer than planned and being supportive the whole time.

Table of Contents

Abstract 2

Acknowledgments 3

Table of Contents 4

List of Tables 7

List of Figures 8

List of Abbreviations 10

Chapter 1; Introduction 11

Chapter 2; Background and Prior Work 14

2.1 Exoskeletons 14

2.1.1 Exoskeleton Uses 17

2.2 Exoskeleton Actuation 19

2.2.1 Passive Exoskeleton Actuators 19

2.2.2 Active Exoskeleton Actuators 20

2.3 Pneumatic Cylinders 23

2.4 Exoskeleton Control 25

2.4.1 Sensors 25

2.4.2 Control and prediction methods 26

2.5 Pneumatic Control 27

2.6 Mechanical Requirements 30

Chapter 3; EC Motor Actuation Testing 31

3.1 Introduction 31

3.2 Design and Methods 31
3.3 Testing Process 34
3.4 Results 35
3.5 Discussion 36
3.6 Conclusion 38
Chapter 4; Pneumatic Actuator 39
4.1 Introduction 39
4.2.1 Hardware Iteration 40
4.2.2 Sensors 47
4.2.3 Software 49
4.3 Controls 50
4.3.1 PID 51
4.3.2 Prediction 52
4.3.3 Simulation and MPC 54
4.3.4 Modifications 55
4.3.5 Velocity 58
4.3.6 Variable Gain 60
4.3.8 Df/dt Control 61
4.3.9 Mode Switching 62
4.4 Final Version Testing 62
4.4.1 Human Subject Testing 63
4.4.2 Final Position Control 63
4.4.3 Stability Testing 64

4.4.4 Position Testing 65
4.4.5 Final Force Control 65
4.4.6 Force Testing 66
4.5 Results 67
4.7 Discussion 71
4.8 Limitations 74
4.9 Conclusion 74
Chapter 5; Future Work 76
Chapter 6; Conclusion 80
References 83

List of Tables

Table 1. Pneumatic Testing RMSE Minimized 70

Table 2. Pneumatic Testing Delays..... 70

List of Figures

Figure 1; Prototype strength augmentation arm exoskeleton [8] 15
Figure 2; Herowear exoskeletons being used to assist lifting [11] 16
Figure 3; The Harmony upper limb exoskeleton [12] 17
Figure 4; BLEEX hydraulic exoskeleton prototype being used for carrying a load [7] ... 18
Figure 5; Electric motor actuated ankle exoskeleton used for reducing the metabolic cost of walking [26] 21
Figure 6; Pneumatic actuator based linear positioning system [56] 28
Figure 7; The motor mount and exoskeleton emulator 32
Figure 8; Exoskeleton emulator design with hypothetical actuator attached (right) and real prototype (left). 33
Figure 9; left, ROS2 software structure and control diagram 34
Figure 10; graph of motor testing on ankle an ankle angle profile with input position and measured position 36
Figure 11, Stepper diverter valve prototype and diverter valve diagram 41
Figure 12; second prototype with DC motors and 4 ball valves with ball valve diagram 42
Figure 13; spool valve prototype and spool valve diagram 43
Figure 14; Improved valve design with internal lines visible to show airflow pathways and the connection for servo control 44
Figure 15; Final actuator hardware design 45
Figure 16; Potentiometer distance sensor (left) and velocity sensor (right) attached to the piston end 48

Figure 17; Force sensor and position locking assembly 49
Figure 18; software structure for testing the pneumatic actuator 50
Figure 19; PID control block diagram 52
Figure 20; Actuator with PID position control 52
Figure 21; Step responses for delay estimation 53
Figure 22; PID position control with overshoot prediction 54
Figure 23; MATLAB simulation of a pneumatic cylinder step response 55
Figure 24; Modified position controller diagram 56
Figure 25. modified position PD controller with prediction 57
Figure 26. cascaded control with velocity inner loop 58
Figure 27. velocity proportional control for ankle angles (top) and a sine wave (middle) as well as the basic control diagram 60
Figure 28. PID Force control for slow sine waves 61
Figure 29. Force control testing, Dfdt method 62
Figure 30. block diagram of the position controller 64
Figure 31; Force testing configuration with fixed rods (left) and springs (right) 67
Figure 32. Stability testing with final controller version 68
Figure 33. Position Control using ankle angle data 69
Figure 34. Force control using ankle moment data 70

List of Abbreviations

EMG Electromyography

PMA Pneumatic Muscle Actuator

ROS2 Robot Operating System 2

PWM Pulse Width Modulation

ADC Analog to Digital Converter

IMU Inertial Measurement Unit

MPC Model Predictive Control

MRI Magnetic Resonance Imaging

PID Proportional Integral Derivative control

SEA Series Elastic Actuator

FDA Food and Drug Administration (US government agency)

IRB Internal Review Board

EEG Electroencephalography

RMSE Root Mean Squared Error

ms milliseconds

EC Electronically Commutated

DC Direct Current

Hz Hertz

Chapter 1

Introduction

Exoskeleton technology was originally motivated by the desire to increase human capabilities in the workplace and in combat. The first popular depiction of an exoskeleton used in combat was the power armor in “Starship Troopers”, a 1959 novel by Robert Heinlein, used to boost the strength and speed of marines while carrying heavy armor. Not long after that in the late 1960s, General Electric prototyped the Handyman full body hydraulic exoskeleton for the US army [1]. While this prototype proved impractical and dangerous, numerous projects since then have improved the concept and delivered promising results for the military and industry. Recent research has focused on injury rehabilitation, metabolic cost reduction, and strength augmentation.

Within the last ten years, exoskeletons have demonstrated practical applications for industry and healthcare. Metabolic cost reduction for walking has been shown in testing in a laboratory environment [2]. Exoskeletons have been FDA approved for rehabilitation of patients with neurological deficit such as those with cerebral palsy or stroke. Commercially available passive exoskeletons in testing can reduce fatigue and perceived discomfort of manufacturing, construction, and agricultural work [3].

Actuation is one of biggest challenges to making exoskeletons a practical technology. While passive exoskeletons can improve efficiency with energy storing elastic components [4], for active, augmentation designs the actuator must have force output, speed, energy storage, and response time competitive with the capabilities of biological muscle which is far more complex and optimized than any human designed technology. So far most of the successful commercialized exoskeleton designs either replace missing muscle functionality in people with disabilities or add passive support [5]. As technology continues to improve it becomes more feasible to augment fully capable human abilities as well, at least in specific situations.

The technologies needed for exoskeleton actuation continue to Improve and become more accessible. Energy storage has advanced rapidly due to electric vehicle research and development, improving options for a fully portable robotic system. Brushless motors are more efficient than older designs and have improved power to weight ratios. Also, portable computing power has increased rapidly in recent years, allowing for improved control of unconventional actuators and more complex methods of human intent prediction using machine learning. Sensors relevant to exoskeleton control, such as electromyography and inertial sensors, are also becoming more readily available and more accurate [6].

This thesis aims to evaluate two actuation technologies in support of the Human Augmentation research grant (Joseph Seay, joseph.f.seay.civ@army.mil) to produce an ankle exoskeleton for metabolic cost reduction. This study first tested a state-of-the-art EC motor from Maxon group to represent the motor technology often used in exoskeleton research. Pneumatic cylinders are a technology that is theoretically

promising but technically challenging to implement and control. The two actuator types were prototyped, optimized, and tested for several parameters to elucidate their capabilities regarding human augmentation.

Chapter 2

Background and Prior Work

2.1 Exoskeletons

Exoskeletons provide a form of human augmentation. Instead of removing human involvement as in robotics, the goal is to improve the capabilities of the human body for some benefit to work efficiency, safety, or quality of life by providing extra torque at the joints. The device typically consists of a rigid frame or soft sleeve which attaches to the body on each side of a joint and an actuator which applies torque in a desired direction. Like robots, they also need to incorporate sensors to measure the movement or intent of the wearer and a controller to respond appropriately. Exoskeleton research is still a new field but many designs and uses have been tested.

Strength enhancement was an early area of research by the military but not initially successful due to limited technology [7]. The goal was for soldiers to move easily with more armor or equipment than otherwise possible [7]. An example of a strength exoskeleton is shown in Figure 1.

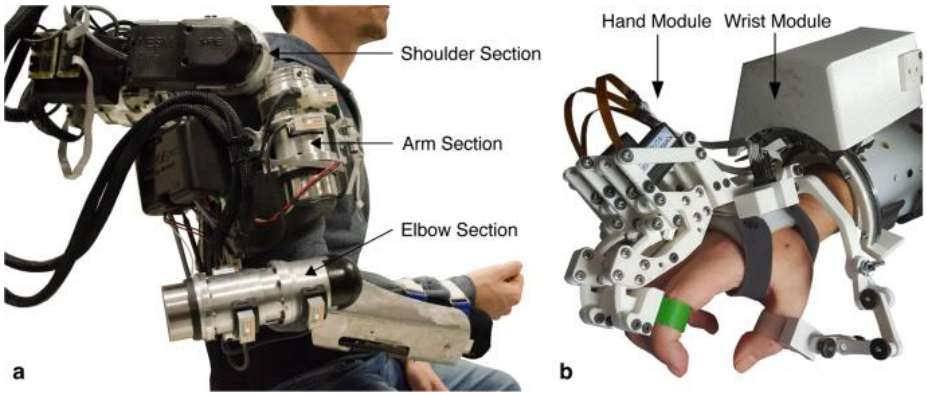

Figure 1; Prototype strength augmentation arm exoskeleton [8]

These have not yet been used in combat due to limited actuator and control technology but effective use in cargo handling has been demonstrated. Strength exoskeletons have also been tested for construction and industrial use [8]. Industrial uses normally do not augment maximum strength but instead reduce the perceived effort of repetitive tasks. One example is an upper limb exoskeleton which assisted manufacturing workers using heavy handheld tools for long shifts [9].

Recent work has moved toward reducing the metabolic cost of movement instead of increasing maximum strength. Malcolm et al. demonstrated reduced metabolic cost for walking using a pneumatic muscle activated during toe off while walking at a constant speed [10]. The goal is for soldiers or first responders to be able to walk faster and further with heavy equipment. This research on the human augmentation project was supporting this goal. These areas of study have encountered problems with motor power and energy storage. Currently available mechanical systems are not as efficient as the human body and struggle to augment ability without tradeoffs such as very short battery life.

Another area of research is for ergonomics and safety in industry. The Herowear exoskeleton shown in Figure 2 is a leading example of this category.

Figure 2; Herowear exoskeletons being used to assist lifting [11]

The passive design provides constant torque to support the hips, shoulders, and back when working in awkward positions. It is marketed to reduce soreness, injuries, and fatigue during manual work [11]. Other designs have been evaluated specifically for overhead work. These could reduce labor costs and injuries in manufacturing.

Exoskeletons are also used for disability rehabilitation. The Harmony exoskeleton, shown in figure 3, is able to help stroke victims re learn arm motor control [12]. A lower limb mobility rehabilitation design called ALEX has also been developed [13].

Figure 3; The Harmony upper limb exoskeleton [12]

Ankle exoskeletons have been used to assist walking in patients with cerebral palsy [14]. Researchers are also experimenting with full lower limb devices for use by paralyzed patients to regain mobility [15].

2.1.1 Exoskeleton Uses

Exoskeletons can be adapted to assist most major flexible joints in the human body. On the upper body, shoulders can be assisted to protect the vulnerable muscles and joint during prolonged overhead work with heavy tools [16]. Arm and full body exoskeletons have been studied for strength augmentation and ergonomics in a factory setting [17]. Therapeutic designs such as the Harmony are also in development. Upper limb designs must have complex linkages around the shoulders to allow for the high degrees of freedom and complex movement pattern in that ball and socket joint. Hand assistance is also being researched. These normally use soft pneumatic actuators to push individual fingers in flexion. This can assist grip strength or encourage motor rehabilitation [18].

Back or torso exoskeletons are normally designed to assist lifting or protect the spine from harmful torsion while bent over. Some of these fix the torso in a rigid position and actuate at the hips while others use a flexible structure fixed at the hips to bend with the wearer [19]. Elastic connections to limbs are common and the goal is normally to apply static forces while holding a position [11].

Lower limb exoskeletons are used to reduce the metabolic cost of walking or improve load carrying ability by providing a force to assist hip, knee, or ankle movement and reduce the workload of muscles [2]. These devices are often intended to improve the mobility and endurance of workers or soldiers who carry heavy equipment. They can also be used to reduce risk of ankle injury or enhance mobility and rehabilitation outcomes for patients with neurological deficit [13].

Full lower limb designs such as the BLEEX prototype, shown in Figure 4, can be used to offset the weight of carried equipment or improve mobility. So far, these have been impractical for real world use due to weight and control difficulties.

Figure 4; BLEEX hydraulic exoskeleton prototype being used for carrying a load [7]

Many other lower limb exoskeletons have been designed to generate torque at individual joints, such as the ankle, knee, and hip. Ankle exoskeletons, in particular, have been studied recently for metabolic cost reduction because the muscles surrounding the ankle contribute to approximately 42% of the total lower limb power during level walking [2]. These devices demonstrate how wearable robotics can reduce metabolic cost during ambulation. For example, Sawicki and Ferris showed how an ankle exoskeleton reduced net metabolic power by approximately 10% during level walking [2]. They used a pneumatic muscle actuator to generate power during push-off phase by activating at a set point in the gait cycle. The Dephy Exoboot can achieve a similar result of reducing the energy of walking using a joint mounted motor [20]. This ankle exoskeleton tracks and replicates the user's ankle angle over several gait cycles, aiding during plantarflexion.

2.2 Exoskeleton Actuation

2.2.1 Passive Exoskeleton Actuators

Passive Exoskeletons do not contribute energy to the wearer with a powered actuator but instead use a purely mechanical system to support weight or store energy in an elastic to apply assistive forces. Human muscles require constant energy input to hold a static force while elastics or springs do not, presenting an opportunity to improve efficiency. The ergonomic industrial exoskeletons would mostly fit into this category such as a back support design [19]. There are also designs to assist holding a load in a set position or while walking [4]. The efficiency of walking or running can be improved with elastic energy storage around the ankles, knees, or feet as well [21].

2.2.2 Active Exoskeleton Actuators

Active exoskeletons, unlike passive versions, use actuators to supply extra power as the wearer moves. These offer more potential for augmentation and rehabilitation but are much more technically challenging. Several different actuation methods have been tested for active exoskeletons, each with some major drawbacks.

Older designs often used pneumatic muscle actuators (PMAs) which use pressure to contract a flexible bag surrounded by woven fibers [22]. This actuation method provides a high force to weight ratio. However, PMAs have a nonlinear response to input and length as well as high hysteresis and fatigue [23]. PMAs are also commonly used for soft exoskeletons such as for hand assistance and rehabilitation [18]. These are normally limited to on/off control schemes and sometimes sliding mode control [24]. Position control has been demonstrated in PMAs but not for exoskeleton use [25].

Zoss et al. designed and built a full lower limb exoskeleton using hydraulic actuators which were able to help the wearer carry a load. The exoskeleton actuates at the hips, knees, and ankles to support loaded walking. It uses impedance control, which is responding to force sensors in contact with the wearer, and switches to a passive state for parts of the gait cycle where low torque was needed. A pump continuously supplies high pressure fluid which is released by servo valves into cylinders mounted around each joint to push a piston, providing linear motion. Hydraulics supply high force output and precise control; however, the components are heavy due to the needed pressure rating. Fluid flow in the system also results in a limited top movement speed,

high impedance while passive, and a lack of compliance to the wearer while providing assistance [7].

Electric motors are the most common method of actuation in current research and commercially available products such as the Dephy Exoboot shown in Figure 5 [20].

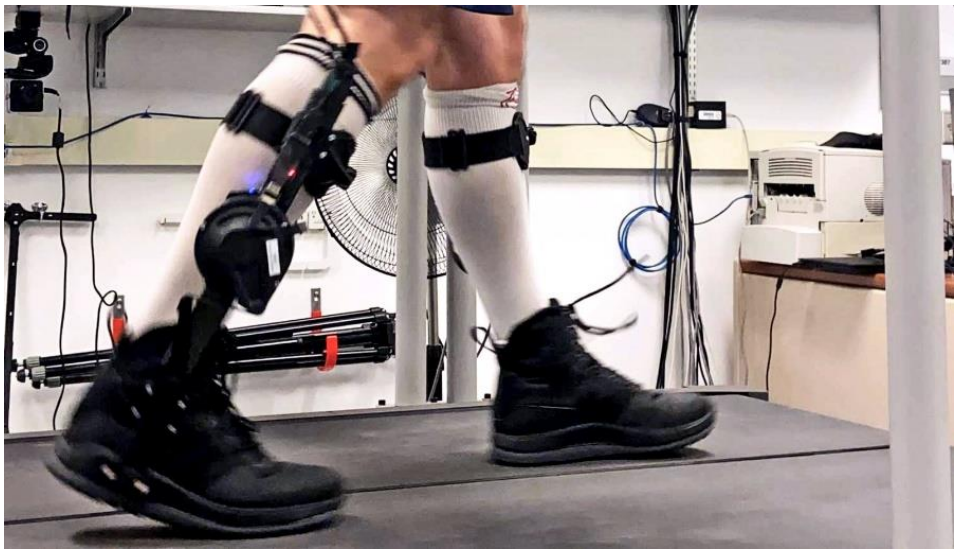

Figure 5; Electric motor actuated ankle exoskeleton used for reducing the metabolic cost of walking [26]

Electric motors have precise controllability, low input delay, and high power to weight. The limitations of electric motors are a fixed top speed which can prevent running ambulation and a lack of compliance to the wearer due to imperfect movement prediction or anticipation. Motors, similarly to large solenoids, can respond to control input in about 30 ms [27]. Normally brushless motors are used for improved efficiency. These can be controlled by pulse width modulation, PWM, for input current or by limiting current. They can achieve accurate position, torque, or velocity control with an encoder for feedback [28]. Motors can be attached directly to the rotational axis of the joint but adding weight to extremities is not always optimal, so other linkages have been tested.

Motors can be moved away from the actuated joint through a Bowden cable system [29]. The motor pulls on an inelastic cable using a spool and the other end is connected to the actuated joint with a moment arm. An outer sheath with compressive strength helps to correctly transfer the tensile force around turns. The Bowden cable design adds friction losses and elasticity but gains improved weight distribution on the limbs or the ability to keep motors away from the wearer's body for testing [30]. These can be used by researchers to test the effect of forces without controlling for a large additional weight.

Linear actuators are another possible mechanical linkage for motors on exoskeletons [5]. They use a ball screw to convert fast rotation into a slow but high force linear motion [31]. The motor and ball screw assembly were mounted on moment arms around the joint similarly to a hydraulic actuator. These can save total weight on a design by replacing the gearbox, spool, and safety stops needed for a direct rotary drive.

Series elastic actuators (SEAs) are used to compensate for some of the limitations of motors. They allow the device to become compliant and fault tolerant. They are used in devices to make the device safer, more compliant to the wearer, or able to store mechanical energy [32]. These require more complex controllers to account for the inherent elasticity and to maintain stability but have demonstrated enough safety to be used in FDA approved medical devices such as the Harmony exoskeleton [12]. Variable spring constant versions of this device have been tested using pneumatics which could address the slower control response and instability created by springs withing the actuator [33].

Shape memory alloys have also been tested for hand exoskeleton use but the actuation time was too slow for practical assistance [34]. Other actuators such as electroactive polymers and linear motors have been considered but are currently not practical for human testing. Linear motors and electroactive polymers have been developed for actuation but are not practical for exoskeletons due to safety or manufacturing difficulties.

2.3 Pneumatic Cylinders

Pneumatic cylinders offer several potential advantages over more common designs and are often used in industrial applications [35]. The design is similar to hydraulic actuation but using a compressible working fluid, normally air. Unlike other actuators they are compliant to the wearer while providing force and have no upper speed limit or overheating constraints [36]. Total work done is limited by the compressed air supply which is not part of the actuator. The limited range of motion provides safety stops which can constrain the exoskeleton to a human range of motion and the cylinder can become passive with low resistance when not powered. A pneumatic system can store energy from a pump over time in a buffer and release it for a higher peak power such as during toe off when walking. Several exoskeletons have been designed to use cylinders such as the Roboknee [37], an overhead lifting assist device [36], and a hip mounted portable device for back assist while lifting [38]. These cylinders can provide assistive force during scenarios when predicting movement is impractical and they sometimes need to let the user move freely. Portable air supplies for pneumatics are not common but have been demonstrated [39].

Pneumatic cylinders have more options for actuating valves and control strategies than hydraulics. Controllers can have simple on/off states, set a target position, or set a target force output. Valves and controllers present the largest design challenge in pneumatics because there are hard design tradeoffs between delay, flow restriction, and flow control. Airflow is also a relatively slow method of transferring energy so systems need to be optimized for delay by removing right angle turns and placing valves near the actuator [40].

The most common valve used in industry is a solenoid spool valve. These have simple on/off control and can allow bi-directional control and position locking. These do not allow for precise flow control or high frequency adjustments so systems using them are 2-state [41]. Proportional solenoids can enable flow control for a PID based positioning system. These are controlled by PWM signals which rapidly adjust the magnetic field holding the valve open [42]. This design allows for rapid flow adjustment but is vulnerable to disturbances and heavily restricts airflow when open because of the short travel distance for solenoids. High frequency solenoids are another approach to flow control where the valve switches between open and closed rapidly and the pulse rate adjusts flow. Pulsed solenoids are more resistant to disturbances but introduce oscillation into the system which can reach the actuator [43].

Servo valves, designed so that a servo motor can turn a ball or needle valve, allow direct flow control. They can also fully open and adjust precisely to minimize flow delay [44]. Actuation can be slower than solenoids because of the motor controller and greater friction in the ball valve. Servos can be attached to a diverter valve to add directional control as well.

The most problematic limitation of pneumatic actuators is controllability. The control response is delayed, highly nonlinear, and difficult to model. The compressibility of air, like a mass spring system, causes oscillation and delayed responses to input which further destabilizes controllers.

2.4 Exoskeleton Control

2.4.1 Sensors

Like all robots, exoskeletons need to sense their environment and respond to input in a useful way. To provide useful assistance, exoskeletons need to sense the movement of the wearer that requires assistance and use that data to follow and provide assistive forces in real-time. Actuation commands also need to compensate for the delay in control systems and actuators to prevent unwanted feedback against the wearer.

Force sensitive resistors or limit switches can be used on the interior of an exoskeleton to detect the wearer attempting to move, as well as the intensity of that movement. Joint flexion and angular velocity can be measured in real time by potentiometers which allows for following the gait cycle or constraining range of motion. Inertial measurement units, IMUs, are another method of measuring motion without mechanical linkages. Each sensor measures acceleration and velocity on three axes. An algorithm can estimate the orientation and position of the sensor based on integrating the data to track body movement [45].

Motion capture technology can accurately map the position of every part of a body in a laboratory setting [46]. This isn’t used for real time control but can improve

prototype testing and the training of machine learning models for control. Systems can use image recognition from cameras or detect retroreflective markers placed on the body for improved accuracy. Force plates combined with motion capture can be used to estimate forces and joint moments within the body.

Surface electromyography or surface EMG is another useful sensor type. These use electrodes on the skin to measure the electric voltage produced by muscles before activation. The voltage is noisy but roughly proportional to muscle activation and it can be detected about 100 ms before force is generated [6]. These signals also vary depending on fatigue and body part.

2.4.2 Control and prediction methods

Early prototypes such as the Berkeley BLEEX exoskeleton used contact force sensors to detect wearer motion and respond [7]. This method is called impedance control and it is simple to implement and versatile for many exoskeleton uses and movements [47]. It can be used in ankle exoskeletons for slow walking but with limitations [48]. All actuators have a response delay and will resist wearer motion during that delay which increases effort, especially during fast movement [49]. Demonstrations of impedance-controlled exoskeletons normally feature slow, deliberate movements instead of natural motor control.

Another simple method of control is to directly respond to a relevant muscle's EMG signal. This is known as myoelectric control. For instance, in one study by Ramos et al., an ankle exoskeleton prototype activated a PMA proportionally to a Butterworth filtered EMG signal from the gastrocnemius to provide walking assistance [24]. Machine

learning based on multiple EMG sensors can predict joint torques in advance for control [50]. Electroencephalography, EEG, has also been studied to predict movement intent by classifying brain activity but it is difficult because of the noise and complexity of brain signals. Several researchers have claimed accurate models for movement intent prediction and this technology is likely to gain more attention because it is also needed for prosthetics and devices for paralyzed patients [51].

Walking assist exoskeletons can be controlled by assuming that a movement pattern is cyclic and timing force inputs for a specific point in the gait. Walking motion can be classified into the swing phase, weight acceptance, and toe off for each foot. The prototype by Sawicki and Ferris provided ankle plantar-flexion assistance during the push-off phase during constant speed walking [2]. The Dephy Exoboot measures ankle angle and calculates a timed ankle angle profile based on the gait cycle [52]. Kinematic models can also predict movement with only position measurements.

Using machine learning with gait measurement inputs anticipates needed actuation based on position control during walking at a variable speed [53]. Position and EMG sensors can be combined in a machine learning model to predict movement which may or may not be cyclic [20]. EMG and gait cycle prediction can anticipate movement with enough accuracy to support metabolic cost reduction out to about 100 ms which sets a maximum target for actuator response time. Finally, it is important for any actuator controller to demonstrate stability to avoid unsafe oscillation feedback.

2.5 Pneumatic Control

Extensive work has been done on position and force control for pneumatic cylinders in industrial applications. These methods could be applied to using a predicted

angle or torque profile for control of a pneumatic cylinder actuated exoskeleton. Pneumatic cylinders are typically used when high force is needed at low cost or when electronics are not safe such as in an MRI room. PID control is a common strategy across many control applications because it is simple to implement and tune but can reject disturbances and maintain stability in a wide range of conditions [54]. Commercially available actuators, such as the one in Figure 6, use PID control to achieve precise positioning or force output, but are limited to low movement speeds because a proportionally higher delay causes instability [55].

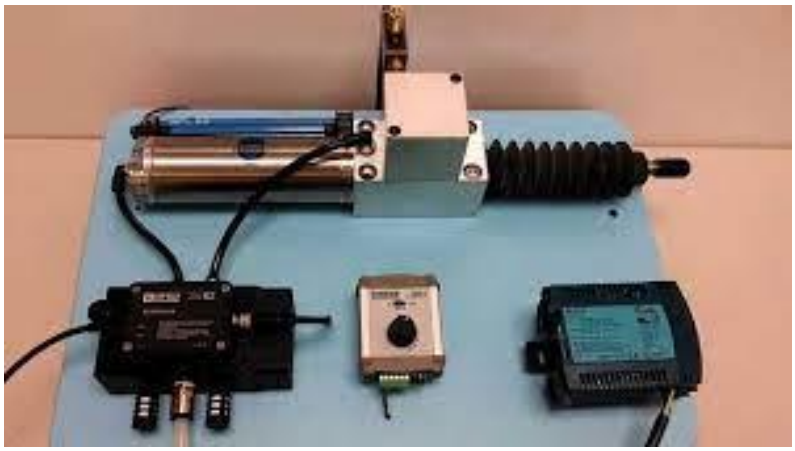

Figure 6; Pneumatic actuator based linear positioning system [56]

More advanced controllers have been developed which use an approximate model of the plant to predict the effect of delay and compensate [57]. Controllers using pressure and acceleration feedback have also been developed by Wang et al. for improved control at high movement speeds. Belforte et al. tested a controller in which the acceleration and velocity control were applied in an inner loop cascaded with proportional position control [58]. Position and force control have also been achieved using admittance methods which involve controlling the derivative of the target measurement [59]. A velocity inner loop was used with discrete pulsed flow valves by

Gaheen et al. [60]. These designs still have oscillation but demonstrate improved stability over position control methods.

Many control designs also switch modes based on position or required accuracy to compensate for nonlinear mechanics. Sliding mode control runs two separate control designs simultaneously and combines the outputs as a weighted average. The weighting of the controllers changes according to a condition such as speed or distance from the target position [25]. Fuzzy logic is similar and adds special conditions to a controller to compensate for quirks of a given system [61]. These are used often for control of PMA devices and are likely to work with cylinder as well [62].

Simulations are often used to validate controllers designed for pneumatic actuators. Simulations can test various levels of pressure, valve flow rates, and friction. These models can determine behaviors and capabilities of a controller but are often incapable of accurately modeling valve flow rate over time due to the complexity of compressible flow. Piston friction models and valve movement are other possible sources of uncertainty [63]. Several papers have shown significant differences between simulated and real results, indicating that pneumatic cylinders need to be physically tested for stability and accuracy claims. Model predictive control is generally not viable for pneumatics because it relies on an accurate model of the system running in parallel with the real system [64]. While accurate full model prediction is not used, it is possible to compensate for delay with a simplified model such as summing control inputs over the delay period or applying a mass spring model for oscillation. Systems with long supply hoses can be controlled more accurately with these methods. These extra control terms can improve accuracy and stability [57].

Force control is similar to position control in that PID is the industry standard method, but other advanced forms exist due to inherent limitations on stability with high delay [65]. For example, force PID becomes unstable easily so multi-valve designs [66] and delay compensation through model prediction have also been developed [67]. Derivative and acceleration control methods, using the rate of change of force as the primary input, have also been used to improve stability but are less accurate controllers during applications with high rates of change.

2.6 Mechanical Requirements

The goal of this study is to determine if an electric motor or pneumatic cylinder can be used to actuate an ankle exoskeleton for walking based on speed, input delay, and control accuracy. Exoskeletons need to be designed based on the mechanical requirements of the joint they are meant to assist. Motion capture and inverse kinematics can be used to determine the movement speed and moment of a joint during certain activities such as walking [68]. 0.1 seconds was considered an acceptable delay when using EMG for prediction based on electromechanical delay tests by Yavuz et al. [69]. The actuator needs to demonstrate stable control above and below the frequency of walking. We chose 5% RMSE as the accuracy target for the total range of motion for control. This amount of error has been shown to affect the level of metabolic cost reduction in a previous study by Sawicki et al.. We hypothesize that the actuator can provide useful assistance for walking based on either position or force control.

Chapter 3

EC Motor Actuation Testing

3.1 Introduction

The initial goal of this project was to test AUBE lab developed ankle angle prediction algorithms on subjects using an exoskeleton emulator in the lab environment. The ankle angle prediction algorithm used machine learning methods to combine sensor inputs from potentiometers, IMUs, and EMG sensors to predict joint angles for the wearer up to 100ms in advance. This should reduce the energy waste and discomfort experienced with impedance control because the actuator delay is compensated for by prediction of future movement. Unlike a controller that assumes a constant cyclic gait, the system should be able to provide a metabolic cost reduction during walking and avoid impeding the wearer during changes in movement patterns such as running or crouching. We hypothesized that the emulator would be able to accurately track inputs from the movement prediction program with a delay of less than 100 ms..

3.2 Design and Methods

A Maxon EC 4-pole 200W motor was selected to power the exoskeleton because it has been successfully used in exoskeleton research before and it is powerful enough to provide the intended assistance without excessive weight [29]. The motor is also designed for a low control delay and low inertia. A 79:1 gearbox converted the motor output to a high torque and low speed rotation needed for actuation.

The motor mount shown in Figure 7 was designed to secure the motor off of the wearer's body and convert the motor rotation into tension on a Bowden cable. The motor was attached to a base plate at several points and had a spool for the cable attached to the shaft. A bike brake cable was used to transfer the tension with one end attached to the outside of the spool and the other on the ankle emulator behind the foot position. The emulator is shown in Figure 8.

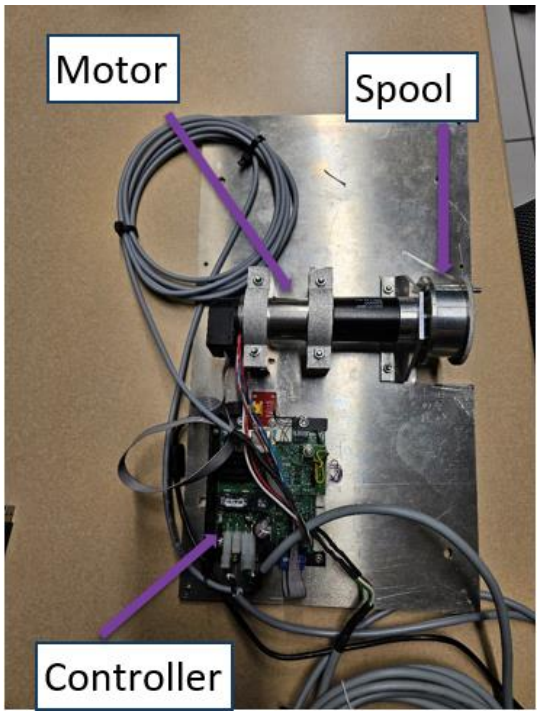

Figure 7; The motor mount and exoskeleton emulator

The emulator, shown in Figure 8 and based on a design by Collins et al., was designed to mimic the mechanics and weight of an exoskeleton and accurately attach to the Bowden cable. It also had a potentiometer on the angle joint for position feedback. The cable could also be attached to a smaller motor on the emulator frame for safer testing.

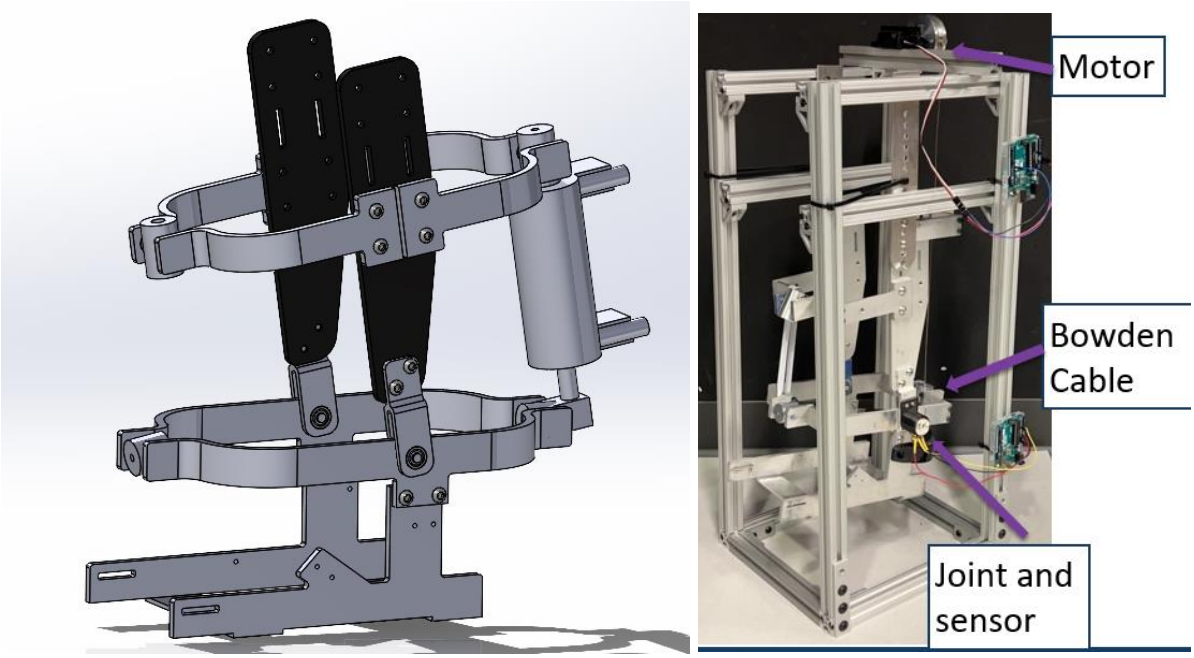

Figure 8; Exoskeleton emulator design with hypothetical actuator attached (right) and real prototype (left).

The motor was directly controlled by an embedded system, produced by Maxon group, that received serial instructions from a computer running ROS2. ROS2 is a robotics focused middleware which allows individual programs to run as nodes and communicate. The exoskeleton system used a measurement node which sent data to the prediction algorithm in another node. The prediction results were sent to the motor communication node which directed the embedded controller and received position feedback. The outer loop position control program was also within this node. A final

node received measured and desired position messages to log and graph them for comparison. A diagram of the control software and method are shown in Figure 9.

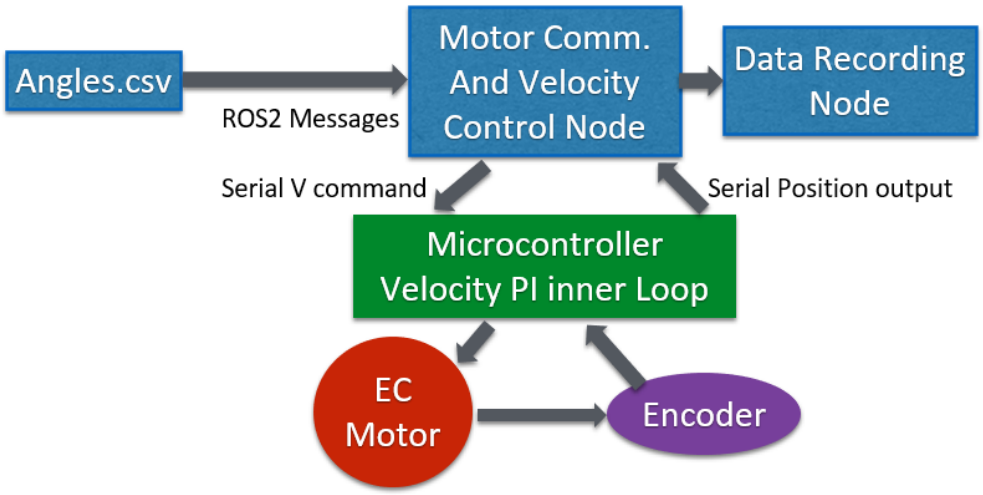

Figure 9; left, ROS2 software structure and control diagram

The motor was controlled using a cascaded control design in which the outer loop running on the computer commanded a velocity to the embedded PI controller proportional to the position error of the motor. The embedded controller used PI control of current input to the motor to reach the target velocity sent. The MAXON controller has several options for input including position, velocity, current, torque, and profiles. The velocity commands were found to be the most reliable and caused the lowest control delay for step responses. The motor measured position and velocity from a built-in quadrature encoder which had 500 ticks per revolution.

3.3 Testing Process

Initial development for the hardware and controls used sine waves for testing. A sample ankle angle profile input at different frequencies allowed for testing controller

stability, accuracy, and delay. The ankle angle data was collected in an IRB approved motion capture session in the AUBE lab. The data collection node calculated an estimated RMSE and a delay which minimized RMSE. For final testing, an open source, recorded ankle angle profile was looped from the input node and motor tracking was looped. The magnitude scale of the data was adjusted to stay within the maximum speed of the motor. Testing was done with default settings on the embedded motor controller. The motor had a spool prototype attached but no Bowden cable or other loading attached.

RMSE and estimated control delay are the quantitative metrics used for motor evaluation. Root mean squared error is the average error for all position measurements compared to the input target position shown in equation [1] where N is the number of samples and x is a position or force value.

$$RMSE = \sqrt{\frac{\sum_{i=1}^{N}(x_i - \hat{x}_i)^2}{N}} \quad (1)$$

The measurement and input can also be offset in the calculation to account for an expected delay value. After data collection, the RMSE was measured for all delay values between 0ms and 200ms. The lowest value was recorded as the RMSE estimate for the system. The delay offset which produced that value was used as the estimated control delay.

3.4 Results

Figure 10 shows the result of testing the motor with ankle angle inputs. The maximum speed of the motor was lower than expected. Within the maximum speed

accuracy was 3.6% RMSE accounting for a 160ms control delay. Delay was estimated based on the graph offset between input and response. Torque output was as high as motor specifications indicated [70]. If velocity was increased beyond the motor limit it undershot the full range of motion of the ankle. Qualitatively, the motor missed some of the sharp accelerations in the motion profile and overshot occasionally.

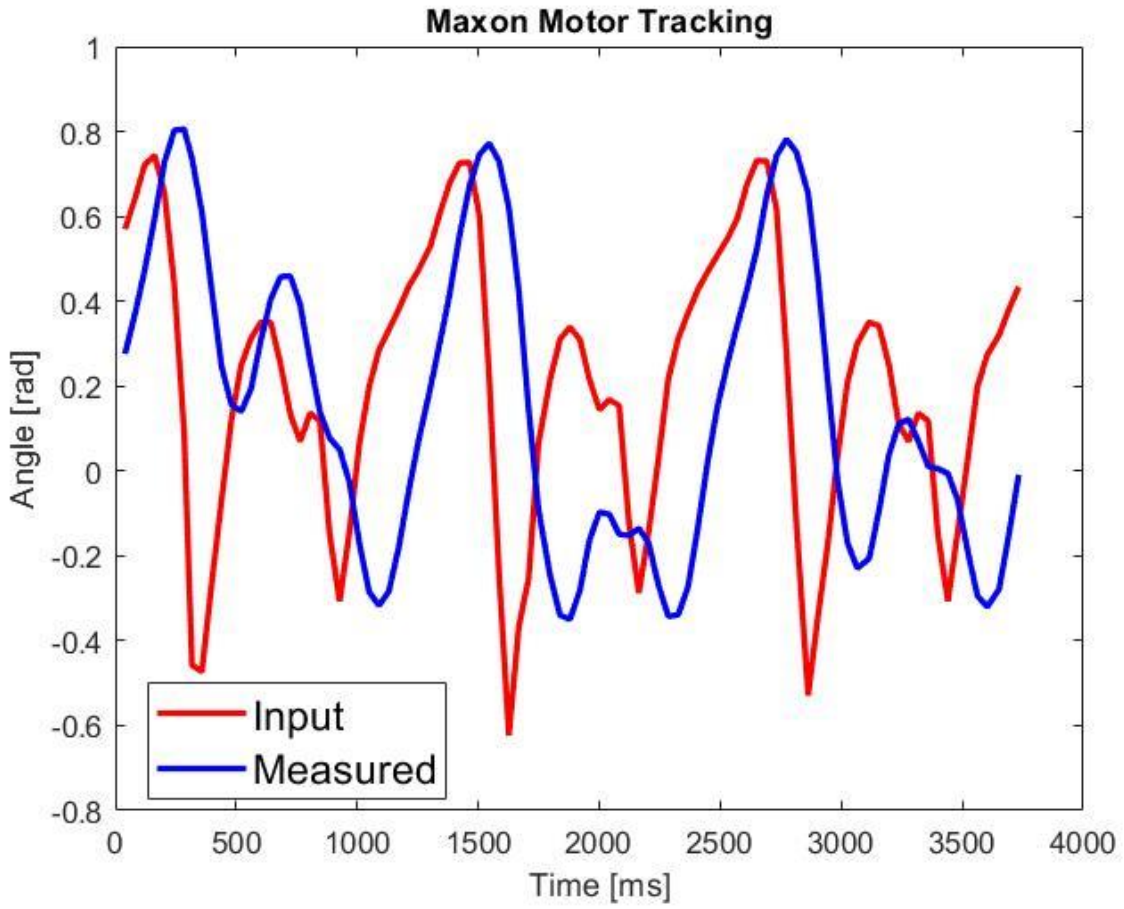

Figure 10; graph of motor testing on ankle an ankle angle profile with input position and measured position

3.5 Discussion

The motor was able to track the motion profile within the intended RMSE but had excessive delay for use of joint angle prediction. The controller never showed evidence

of instability or excessive oscillation. The motor was able to meet the maximum angular velocity of the ankle angle profile but appeared to lag on angular acceleration. It was able to rapidly switch direction and speed which makes control simpler than with a less responsive actuator.

The motor comes with several limitations for this application. It has a hard limited top speed which was lower than expected. A gearbox had to be selected which determined the speed and torque limits to fit all intended motion which costs torque during the toe-off phase of walking for a given motor power and weight. The motor appeared to reach its maximum speed to match this walking profile so adjusting the actuator for other movements such as running would be difficult. The motor is also not compliant or back drivable by the wearer which can result in extra effort or tripping if movement prediction is not highly accurate (> 5% RMSE). Movement intent prediction has not yet been perfected and this is likely why commercially available exoskeletons still use impedance control or have limited functionality.

Motor testing and development also raised safety concerns. Errors in software or position measurement sometimes caused the motor to run at full speed and power for a few seconds when started. The motor, drivetrain, and emulator did not limit the range of motion of the ankle so there was risk of full motor torque being applied to a human ankle in an overextended position if human testing was ever attempted. This problem prompted projects to design safety stops and a new actuation method.

These concerns also point to limitations in the study. The motor was not connected to a real human wearer or even a source of mechanical resistance. It was tested on a single movement from one subject, so the study does not represent all

possible human biomechanics, even for walking. The motor testing requirements also depend on a motion prediction algorithm which was not complete or evaluated at the time of testing. Due to the delay in communication between the Maxon controller and the controlling computer, found to be about 40ms per cycle, the results probably do not represent the physical limitations of the motor and instead represent a highly delayed discrete controller which would have limited accuracy on highly dynamic data even with a theoretically ideal motor.

3.6 Conclusion

Motor testing was mostly successful but exposed limitations of the motor and prompted development of an alternative actuation method. Electric motors will always be a popular option because they are simple to implement and have the best energy efficiency of any actuator from battery power. They are most effective in cases where impedance control is usable or where movement is accurately predicted.

Chapter 4

Pneumatic Actuator

4.1 Introduction

A pneumatic cylinder was selected as the alternative actuation method to overcome the limitations of the Maxon motor. In theory they have a force to weight ratio, no speed limit, compliance, and safety at the cost of more difficult control. Position and force control were tested for the pneumatic actuator because there is more successful research for force control and joint torque prediction is also being researched. We hypothesized that the pneumatic cylinder could meet goals for force, speed, delay, stability, and accuracy while being controlled for position or force.

4.2 Design Process

Finding the size, placement, and power requirements for a pneumatic actuator is relatively straightforward. The main challenge for using this actuator is achieving precise control of position or force especially with low cost, commercially available components. First, the hardware was iterated to an optimized version based on the criteria of response delay, flow control, and flow restriction. Response delay is the time between

sending a signal to the motor on the valve and measuring a response in the system. Flow control is the ability to limit airflow accurately and quickly by adjusting the orifice size while flow restriction is determined by the maximum orifice size and limits the maximum speed and effective load of the actuator. After hardware was optimized, software was designed to make use of the final hardware version to achieve the best control accuracy and stability.

4.2.1 Hardware Iteration

The control hardware was built onto a double acting cylinder so each side needed to have input, exhaust, and closed settings with precise flow control. Valves were attached directly to the inputs to minimize flow delay. For all prototypes, the motors were attached to valves using 3D printed adapter components designed in Solidworks. Prototypes were tested in a polycarbonate box due to safety concerns.

In industrial applications, pneumatics are normally controlled using solenoid valves which are made in single valve or multi input spool valve configurations. These were never tested because most are designed for on/off control only and proportional solenoids are vulnerable to disturbances and oscillation which would limit accuracy. These valves also have high flow restriction because of the small range of motion of solenoids which would increase response delay. Many spool valves are also two stage designs, using a small valve to release pressure which pushes the main valve, which prevents proportional control and increases delay. Motors appear to be a more robust solution for precise flow control.

The first version, shown in Figure 11, used diverter valves driven by stepper motors. Diverter valves were used to reduce weight and complexity by controlling multiple functions with a single motor. Steppers were selected for high position control accuracy. This version mostly failed to operate because the stepper motors lose torque while moving quickly which made control responses slow and unreliable. The steppers also failed to keep track of their valve position over time. The diverter valves were also not an ideal choice because they restricted flow when open and were completely closed for a wide range of positions which caused the actuator to lock in position for >200 ms when switching direction. Later, the steppers were replaced with servo motors which improved the reliability of the system but did not address the dead zone caused by diverter valves.

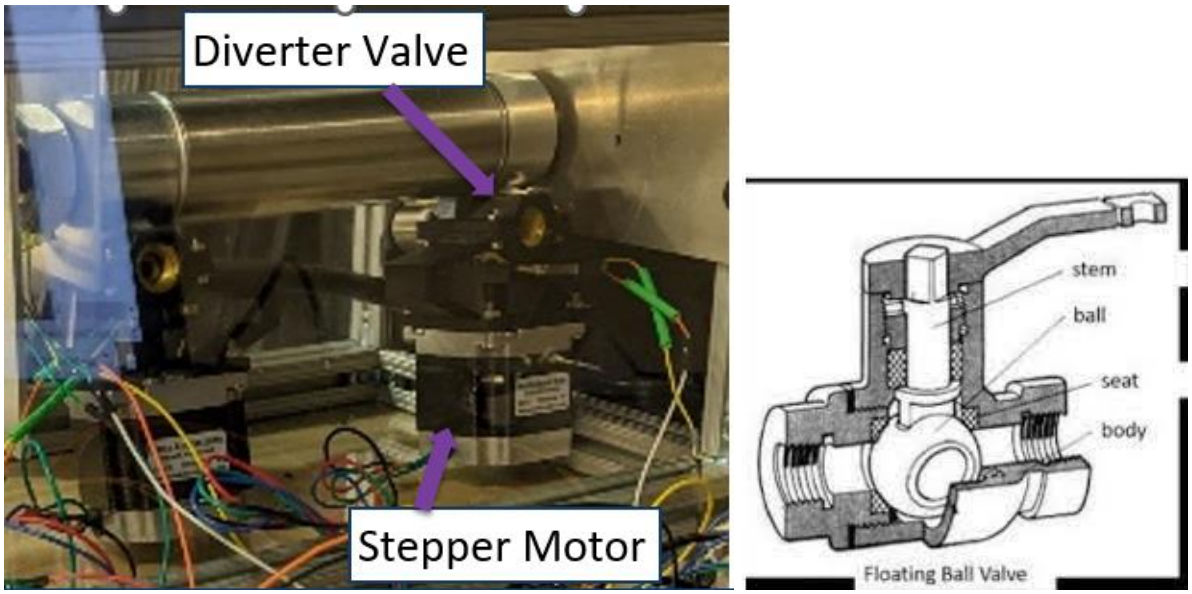

Figure 11, Stepper diverter valve prototype and diverter valve diagram

The next version of the actuator, shown in Figure 12, used four individual ball valves attached by T junctions, making an H bridge configuration, to avoid the dead zone of the diverters. DC motors were used because they have no software delay and a

high movement speed. This design was able to actuate quickly and with less delay but was impossible to control even for a sine wave input. There was no direct position feedback on the valves which increased control instability. The software attempted to use speed and acceleration to estimate valve positions, but it was too inaccurate. Backlash in the motor gearboxes worsened this problem and delay. The valve H bridge worked but actuation speed was still a concern.

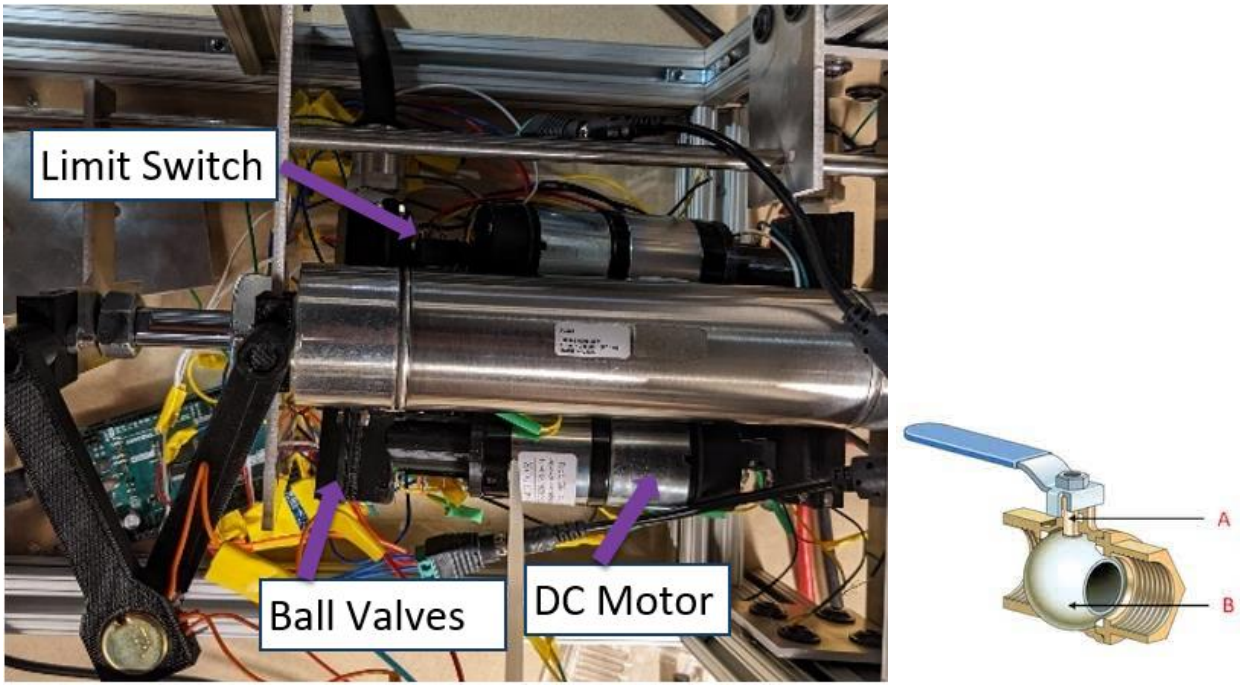

Figure 12; second prototype with DC motors and 4 ball valves with ball valve diagram

The third iteration, shown in Figure 13, used spool valves in an attempt to reduce the range of motion for actuation. Servos were settled on as the motor for valve actuation because they are a good combination of speed, torque, and precision. The valves used linear motion of a spool to control airflow between input and output without the large dead zone of the diverter valves. The limitation of this design was flow

restriction when fully open. Stable control was far easier with such restricted flow and precise control, but the actuator would not meet speed or force output requirements.

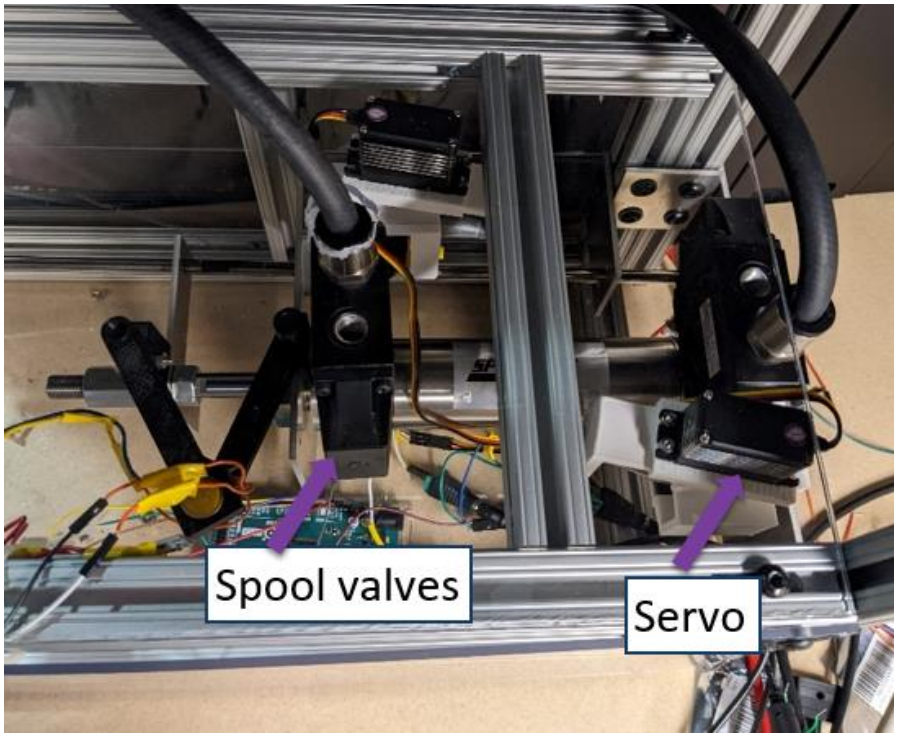

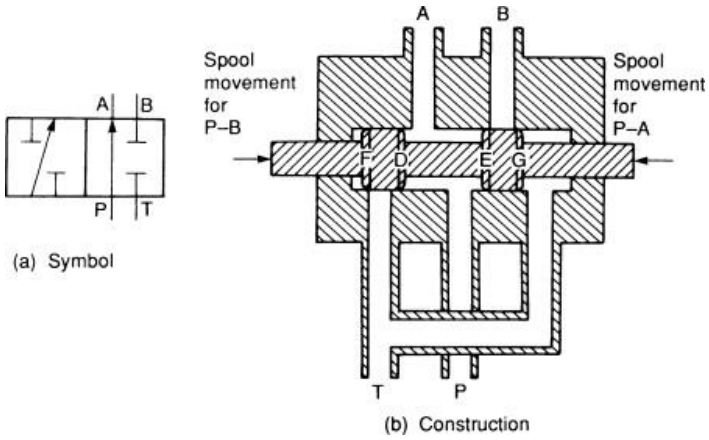

Figure 13; spool valve prototype and spool valve diagram

A new valve was designed to explore optimizing for precise and fast actuation. The design, shown in Figure 14, was not manufactured but was used to estimate the possible hypothetical improvement over current valves with greater resources. The

cylindrical valve ball is servo actuated and has two separate airflow channels at right angles to each other which connect the cylinder to pressure input or exhaust. This is intended to gain the benefit of a diverter valve with the open airflow characteristics of two on/off ball valves. The fully closed range is only about a degree wide around 45 degrees, preventing significant locking while switching direction. Using only a quarter turn for the range from full exhaust to full input should also improve response time. Sharp turns in the airflow paths are minimized to allow for the fastest possible airflow. The servo mounting hardware is similar to the real prototypes. This design was considered not manufacturable with machining or additive manufacturing.

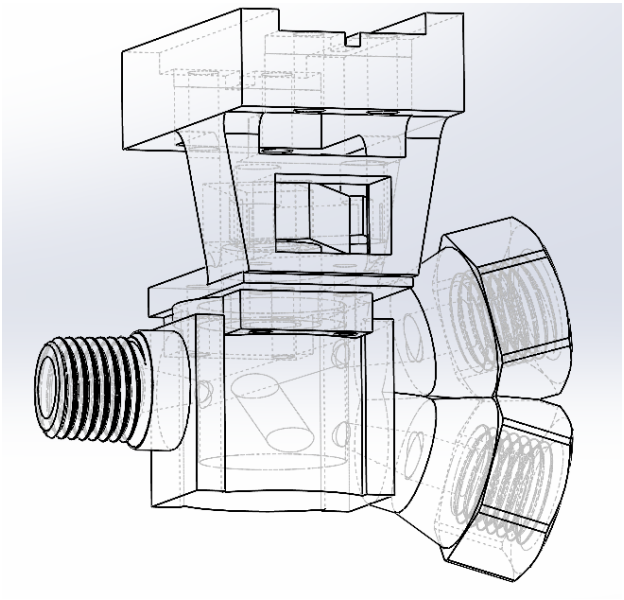

Figure 14; Improved valve design with internal lines visible to show airflow pathways and the connection for servo control

The final version, shown in Figure 15, reverted to the four ball valve H bridge configuration but used servo motors for actuation. Switching to digital servos, (Hitec D940TW), reduced their control delay to an insignificant amount compared to DC motors. The junctions between valve pairs were switched to Y shaped parts because

right angles cause flow restriction and add response delay. This design had the lowest flow restriction and response delay while still allowing flow control. Servo motors were also tested and selected for the lowest delay while actuating the valve. An IMU was attached to the motor arm to detect acceleration. The motor and IMU were connected to the same microcontroller so that the delay between motor activation and servo movement could be recorded. The servos used had a delay of about 30ms.

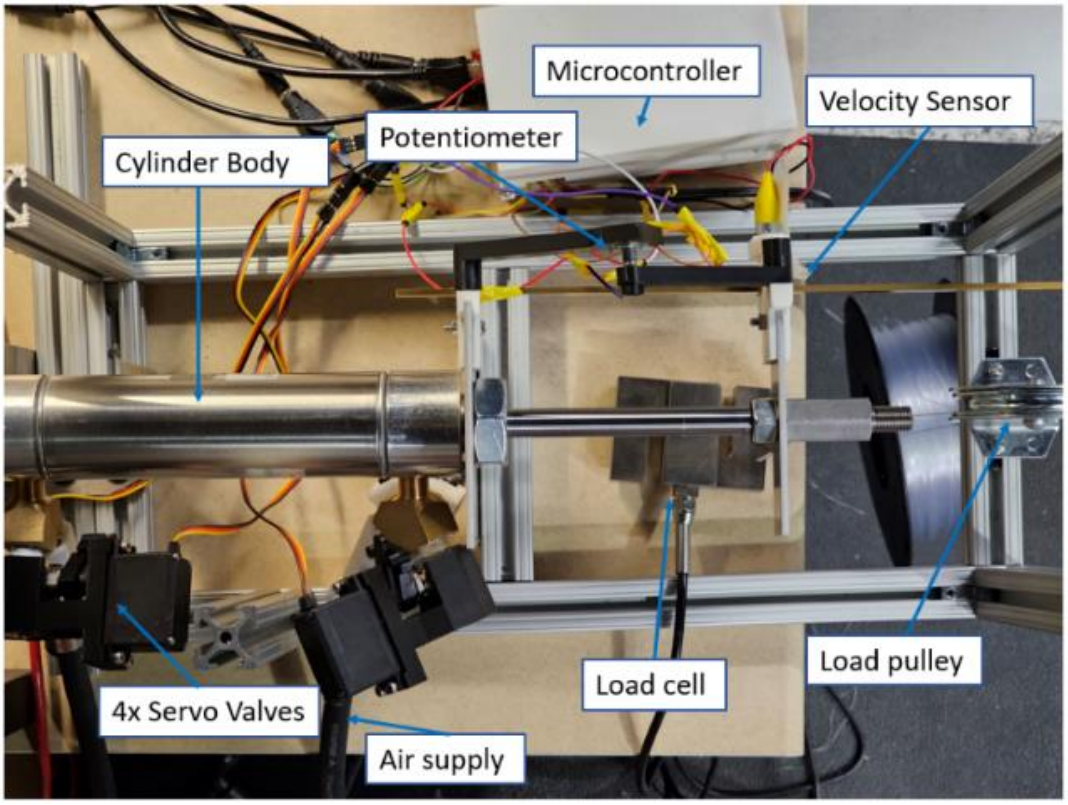

Figure 15; Final actuator hardware design

In order to provide the needed assistance with the finalized control hardware the final version of the actuator, shown in Figure 15, was built around a double acting pneumatic cylinder with a 1.75-inch bore and 4-inch stroke. This cylinder was sized to provide approximately 20% of the maximum ankle moment with a 7 cm moment arm. As a result, the design should provide ~440 N of force based on the work by Hansen et al.

[71]. The moment was obtained from a reference design used in the Auburn University Biomechanical Engineering (AUBE) lab shown in Fig. 2. This design is based on an exoskeleton prototype by Zhang et al [29]. Sizing was based on (2) and typical time responses for compressed flow [66]. Force production of a pneumatic cylinder is shown in (1).

$$F = p_1 A_1 - p_2 A_2 - ma \tag{2}$$

In this equation, F is the force produced by the piston, p is the pressure on each side, $A1$ and $A2$ are the areas of each side of the piston head, a is the piston acceleration, and m is the piston mass. This maximum force needed to be provided at approximately 50 psi so that there was still a greater than 50 psi pressure difference from the air supply to keep valve mass flow rate high enough for the maximum movement speed. Based on that estimate the cylinder needed to have an internal area of over 2 square inches and move at over 40 cm/s. The design included four servo valves, (Hitec D940TW), built around ¼ inch ball valves attached to control pressure input from a source and exhaust to atmosphere for each direction of motion. The valves were sized to allow enough mass flow rate of air at a 50-psi difference for motion at the intended top speed based on (3) and (4).

$$\dot{m} = \gamma p_s \sqrt{\frac{k}{RT}} A \tag{3}$$

$$\gamma = \sqrt{\frac{2}{k-1}} \left(\frac{p_s}{p_e}\right)^{\frac{k+1}{2k}} \sqrt{\left(\frac{p_s}{p_e}\right)^{\frac{1-k}{k}} - 1} \tag{4}$$

In (2) and (3) $\dot{m}$ is the mass flow rate of air, p is pressure for the source and exhaust, k is a heat capacity constant, R is the ideal gas constant, A is the piston head area, and T is the temperature of the source gas. The flow is assumed to be unchoked and through

an orifice in a plane [63]. The maximum angular velocity of an ankle during walking is 5.5 rad/s based on motion capture work by Mentiplay et al [68]. This equals a movement speed of 35.5 cm/s for the actuator with a 7 cm moment arm. Based on these equations a ¼ inch valve can allow the cylinder to extend at the maximum speed while at 50 psi assuming a source over 100 psi.

4.2.2 Sensors

The actuator also has difficult sensor requirements. It needed precise updates on position, velocity, or force output at above the operating frequency of 120hz without significant noise for feedback control to be effective. Position was the first measurement implemented and initially used a time-of-flight sensor. This was mechanically easy but produced a noisy measurement. Potentiometers wired to an ADC can produce the most accurate measurements but are normally rotary. This was addressed by using 3D printed lever arms, shown in Figure 16, to spin the potentiometer from linear motion. This also accurately represents the measurement of an ankle angle with the actuator mounted, avoiding a nonlinear distance to angle conversion in software.

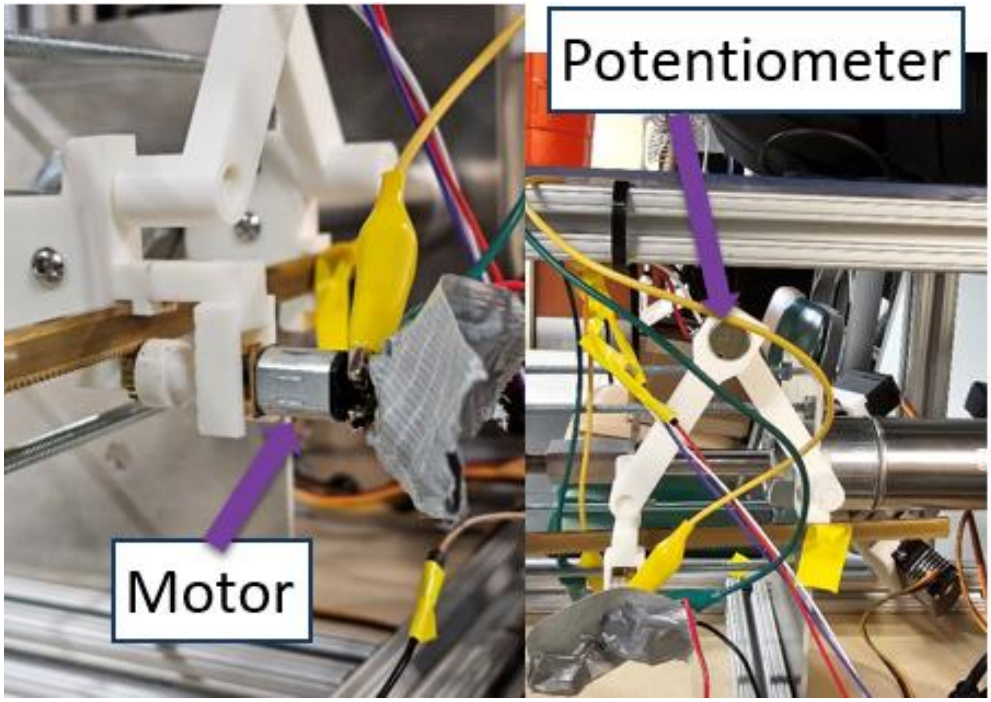

Figure 16; Potentiometer distance sensor (left) and velocity sensor (right) attached to the piston end

Velocity was first calculated by deriving the position measurements, however these values had noise and sudden jumps caused by the discrete nature of the position measurements. A rack and pinion was added alongside the piston to convert movement to rotation for a sensor. First encoders were used but low-cost versions did not have the precision to improve over position derivation. The final sensor used was a small DC brushed motor with a back EMF sensor. A 5V, 16-bit ADC, connected to the Arduino Mega, was used to measure the generated voltage from the motor, from the negative terminal. The positive motor terminal was connected to a 2.5 V source, allowing the ADC to measure positive and negative velocity. Another voltage divider was added to keep the maximum voltage measured below 2.5 V. A capacitor was added to smooth noise caused by motor commutation. The new sensor was checked against derived

position to verify measurement accuracy. The final version is shown in Figure 10 below the position sensor.

The force sensor is an S type load cell shown in Figure 17. The Arduino interfaced to the microcontroller with an amplifier and ADC module from Sparkfun. The load cell was attached to the piston on one end and the locking plate on the other. This plate could be connected to the cylinder body by fixed threaded rods or springs.

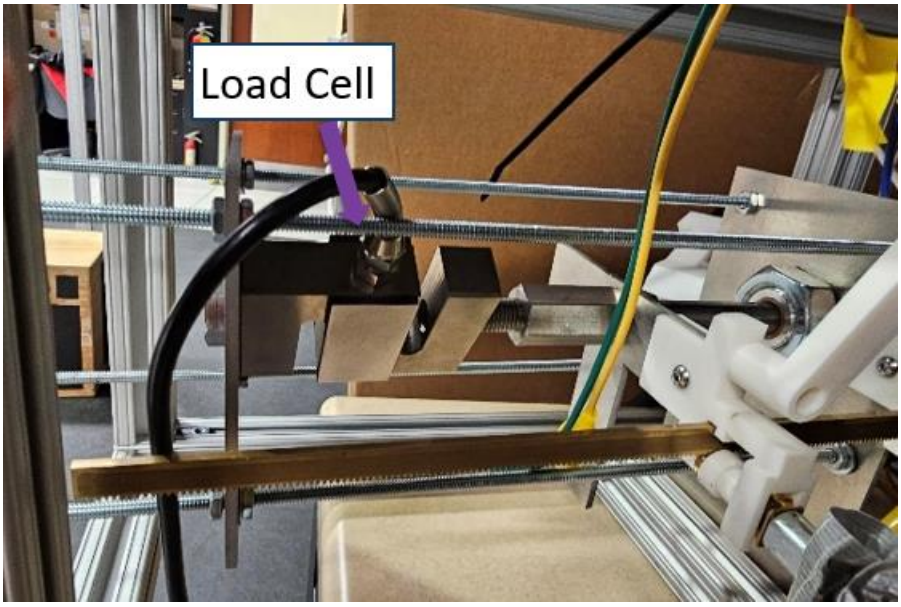

Figure 17; Force sensor and position locking assembly

4.2.3 Software

The feedback controller was coded onto an Arduino Mega. The controller communicated with the computer over serial for input positions and results logging. These computer functions were each handled by ROS2 nodes similarly to the Maxon motor. One node read .csv files of recorded motion capture data while the other node logged input positions and data from the Arduino to .csv files for analysis and graphing in MATLAB.

Within the microcontroller, measurements and inputs were used by the feedback control algorithms described below. The controller outputs a number called C in code which determines valve action. For both the position and force controllers, the C value is translated into position commands for each of the four servo motors. One diagonal pair moves to the closed position while the active pair opens proportionally to the control value, allowing for pressure input to one side of the piston and exhaust from the other. Figure 18 shows a diagram of the software and communication hardware used.

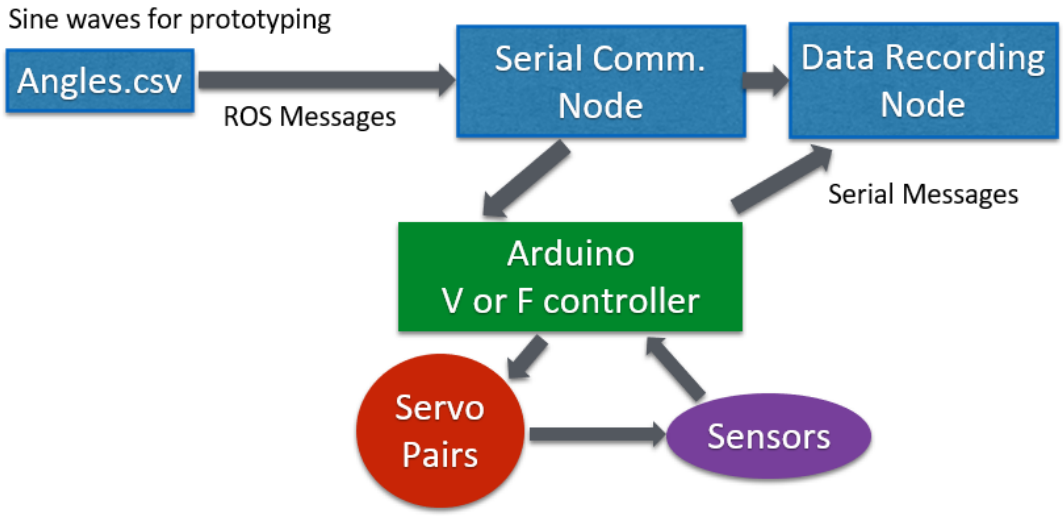

Figure 18; software structure for testing the pneumatic actuator

4.3 Controls

With hardware and communication finalized, a feedback controller was developed to control airflow in and out of the cylinder by operating the servo motors. This software, running fully on the microcontroller, needed to correctly account for sensor input, delay, and performance goals. All the controllers operated at 120hz using

a sine wave input. 2hz was targeted for the sine inputs but for several controllers a slower input was needed to see stable control.

4.3.1 PID

PID control is an industry standard method of feedback control in many applications. There are commercially available pneumatic positioning and force application systems using this method. The name PID refers to Proportional Integral, Derivative as shown in a Simulink block diagram in Figure 19. The controller applies proportionally to error, to the integral of the error over time, and inverse to the derivative of the error. For this controller the integral component had saturation limits while the derivative was unfiltered. These components allow the controller to respond quickly, reject a first order disturbance, and damp oscillation. Despite this, PID applied to this actuator suffered from oscillations and instability as shown in Figure 20. A difference appears to be that the commercial systems have small, flow restricted valves, normally solenoids, and slow movement speeds relative to cylinder length as a result. This results in the system delay being low relative to the total time to complete a movement, ideally less than 10%. PID controllers become ineffective with low bandwidth and high relative delay because these can cause high overshoot and integral oversaturation, which is when the error integral continues to grow during the delay period causing positive feedback in oscillation. This prototype could actuate its entire length in under 200ms while the delay was about 100ms. Increasing damping or adding mechanical damping did allow for rough tracking of a slow sine wave but still with regular overshoots.

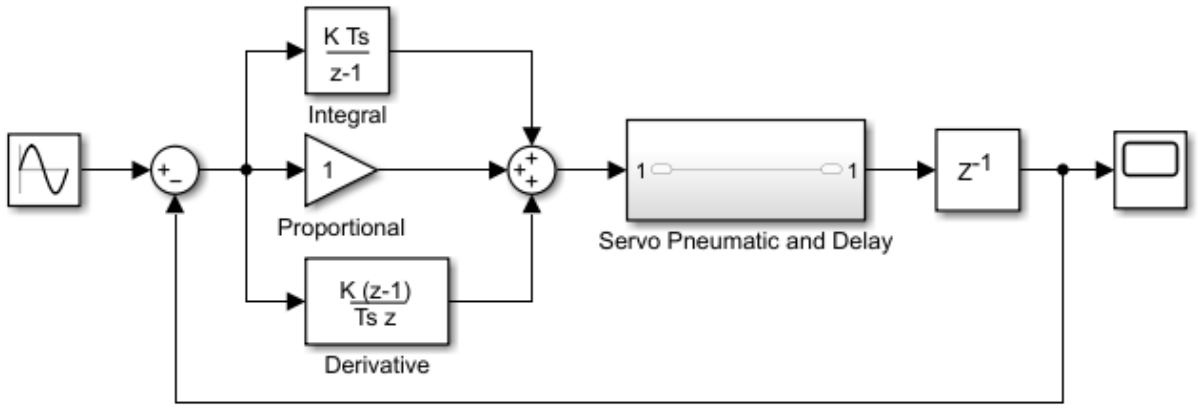

Figure 19; PID control block diagram

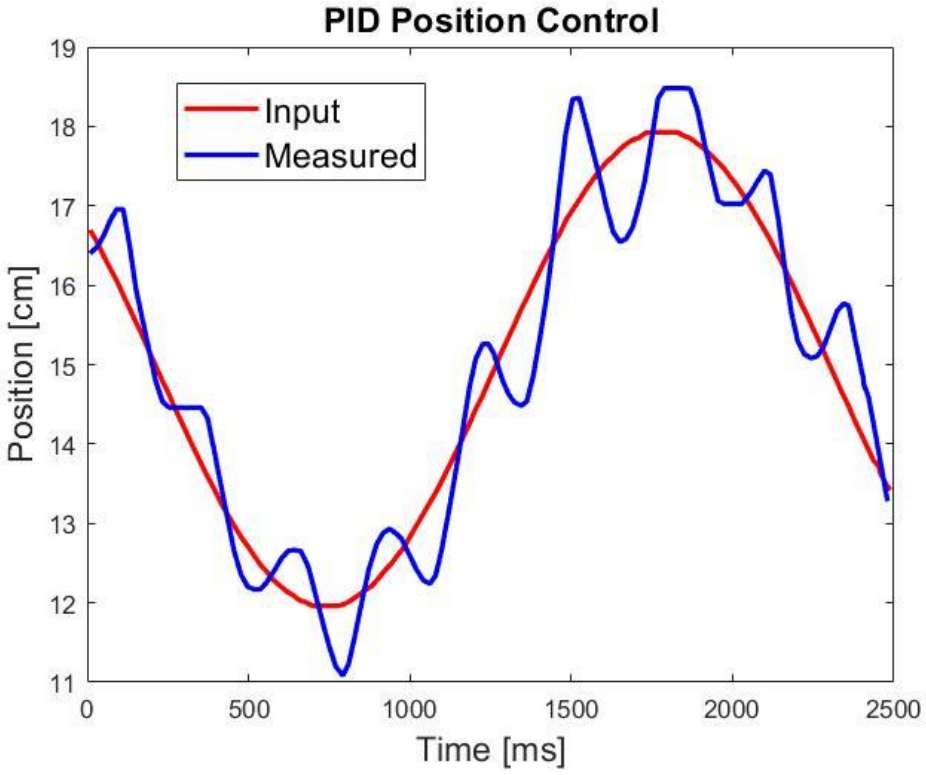

Figure 20; Actuator with PID position control

4.3.2 Prediction

After PID failed due to excessive delay, the next step was to add prediction to compensate for this delay to stabilize the system and reduce overshoot. The first simple

approach was to add the measured velocity multiplied by the estimated delay period to the measured position for control feedback. The sum of control inputs over the delay period with a multiplier was also added to the measured position to further improve prediction. This method did reduce overshoot and improve the capabilities of the actuator. The problem with this approach was that the delay period varied with conditions and input and the effect of control input was never perfectly consistent. Delay was estimated from step responses, shown in Figure 21, but this was not reliable. The prediction multiplier could never be tuned accurately. The nonlinear and complex behavior of valves limited the effectiveness of a linear prediction approach. Figure 22 shows the result of adding prediction.

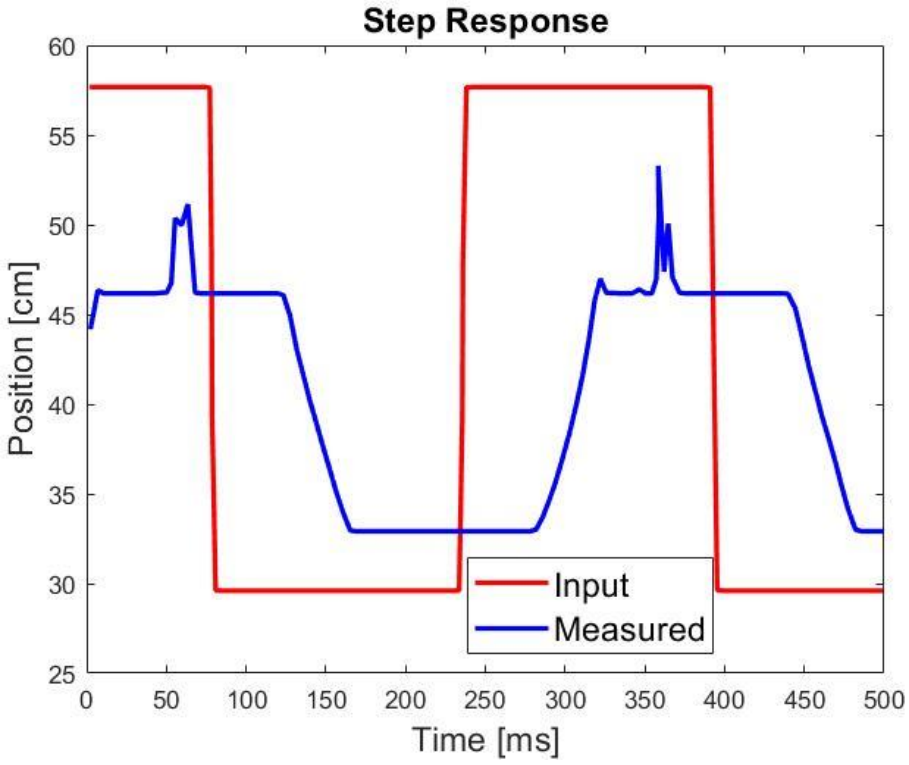

Figure 21; Step responses for delay estimation

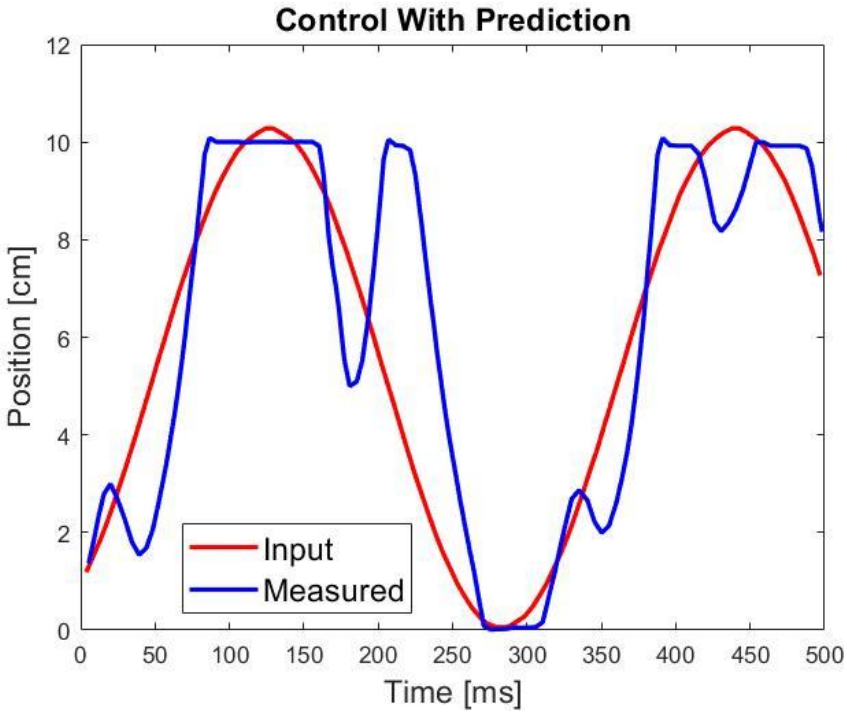

Figure 22; PID position control with overshoot prediction

4.3.3 Simulation and MPC

In order to try more advanced control strategies, a model of the system plant was needed. This would have also improved the speed of controller testing. A simulation was made in MATLAB initially based on the same force and flow equations used for component sizing. Extra functions were added to account for the mechanical limitations of valve actuation and airflow delay. A step response was tested using the sim and shown in Figure 23.

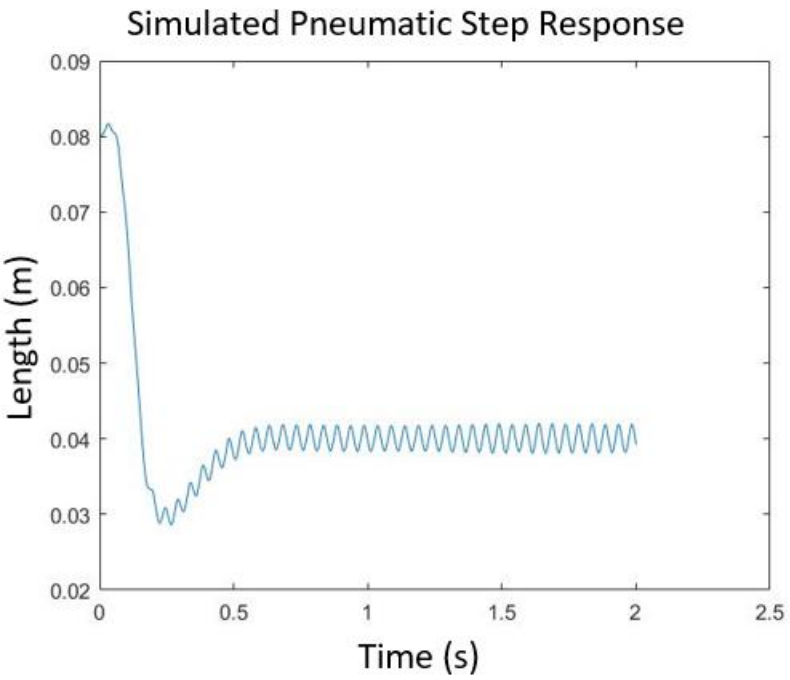

Figure 23; MATLAB simulation of a pneumatic cylinder step response

The simulation showed somewhat physically realistic behavior for a cylinder but it was not able to match the timescales or magnitudes observed in the real system. A high frequency oscillation was never seen in the real system either. This result is consistent with other papers showing simulation in that the model was not accurate enough to be useful for safety analysis or controller development.

4.3.4 Modifications

Several other modifications improved the performance of the controller. A diagram of the modified design is shown in Figure 24.

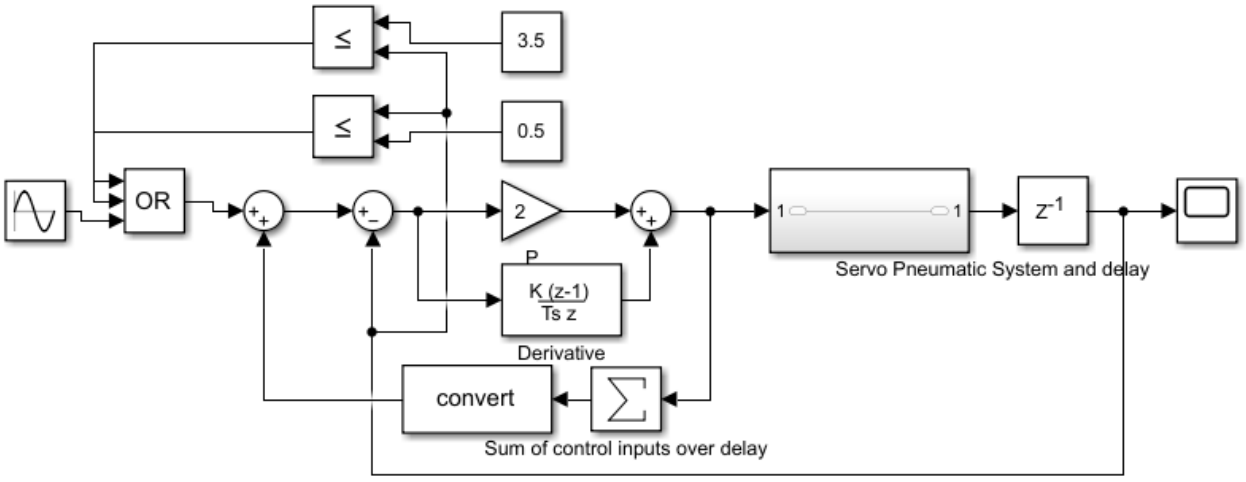

Figure 24; Modified position controller diagram

Removing integral control made it less sensitive to delay and more stable. This is a common suggestion for high delay systems although it reduces accuracy. A separate mode was added which activates when the piston is within 0.3 inches of a stop and sets the target velocity away from the stop. This mode switching function reduced slamming into the ends and prevented “wall hugging” which appeared in many versions of the controller, especially velocity-based designs. The best results are shown in Figure 25.

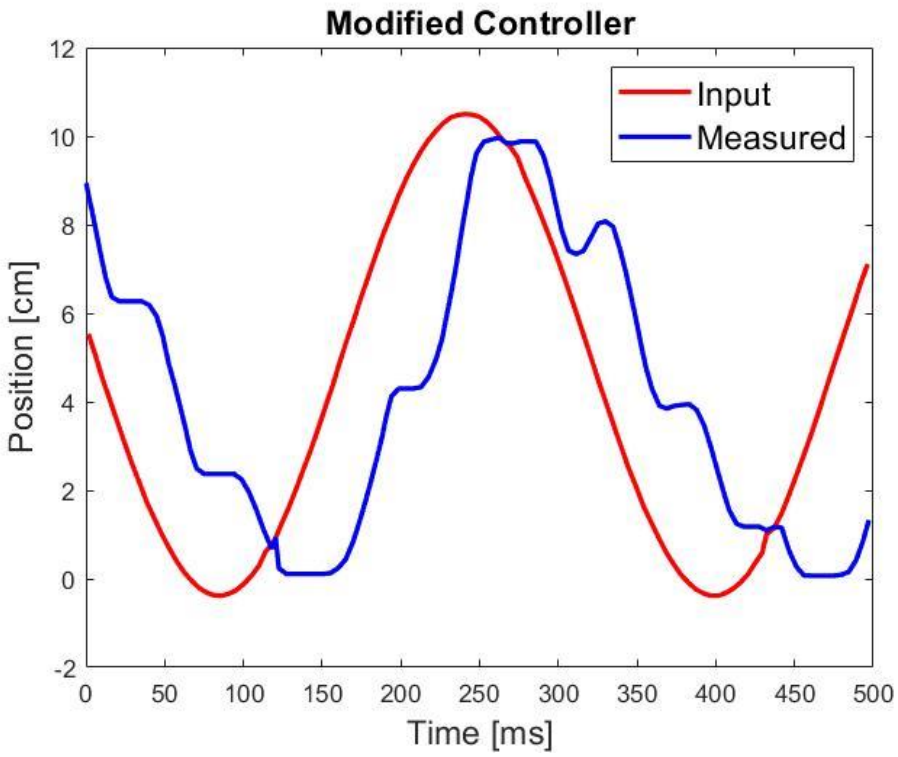

Figure 25. modified position PD controller with prediction

Another design explored, shown in Figure 26, was a cascaded controller with a proportional velocity inner loop. A target velocity was set based on position error which was then controlled for using the velocity sensor. This method did not produce a significant improvement and often increased the response delay of the system. According to control theory, the inner loop needs to have 10x the bandwidth of the outer loop for this design to be effective. This was difficult to measure but probably not the case for the system since both depended on the same servo valve actuators.

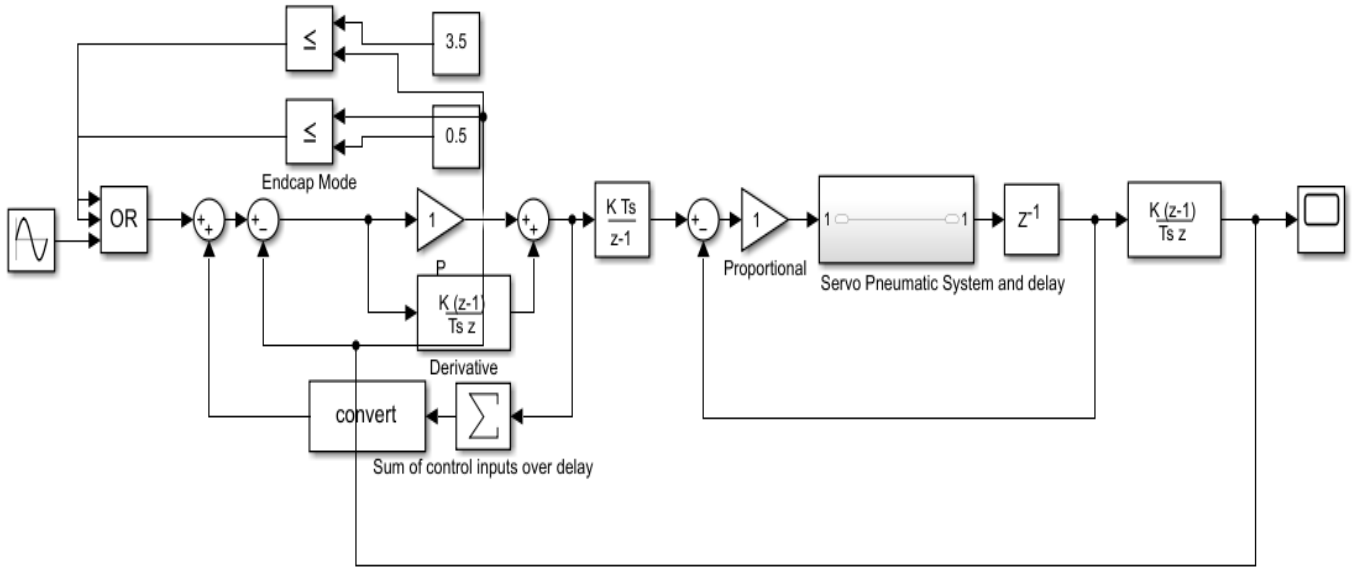

Figure 26. cascaded control with velocity inner loop

4.3.5 Velocity

The largest improvement in the controller design, shown in Figure 27, was achieved by removing direct position feedback and replacing it with velocity. Input positions were derived to desired velocity. Proportional control was used with the velocity sensor measurements. Overshoot prediction was also used based on the sum of control inputs. Unlike every other design, this controller remained stable in all conditions and closely matched the velocity profile of the input. Position bias was high and not consistent and any attempt to add partial position feedback also brought back instability.

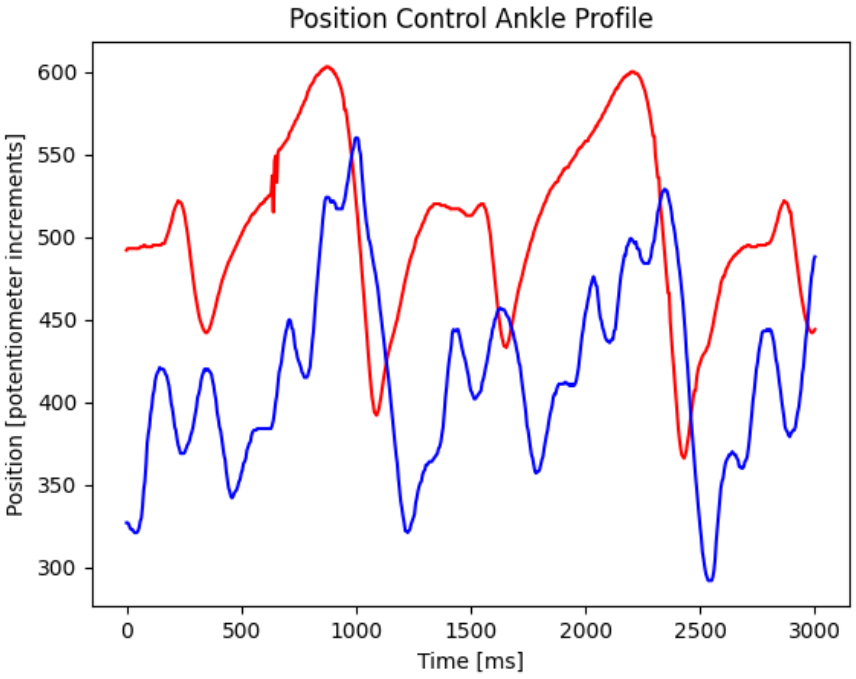
Position Control Ankle Profile
Position [potentiometer increments]
600
550
500
450
400
350
300
0
500
1000
1500
2000
2500
3000
Time [ms]

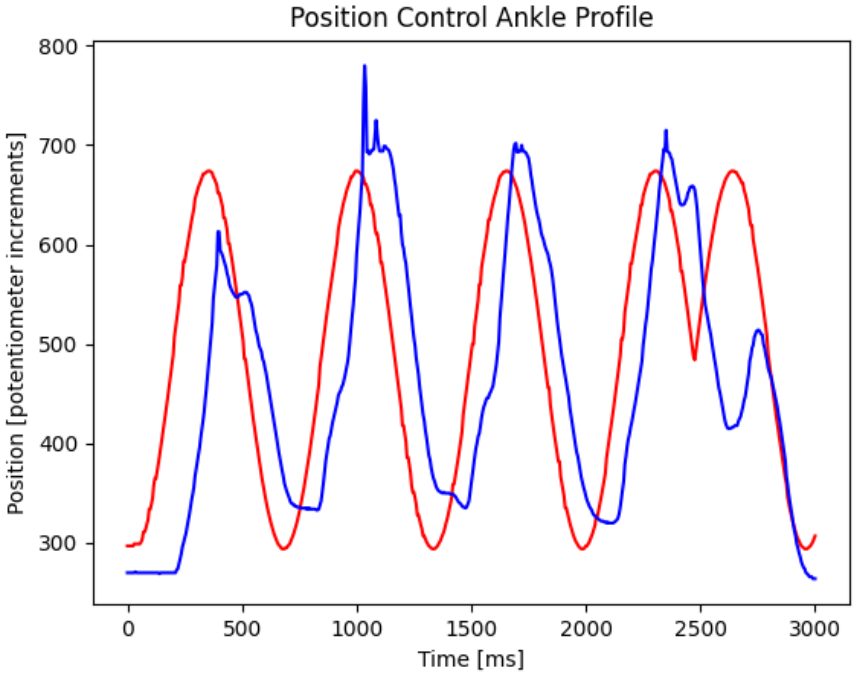
Position Control Ankle Profile
Position [potentiometer increments]
800
700
600
500
400
300
0
500
1000
1500
2000
2500
3000
Time [ms]

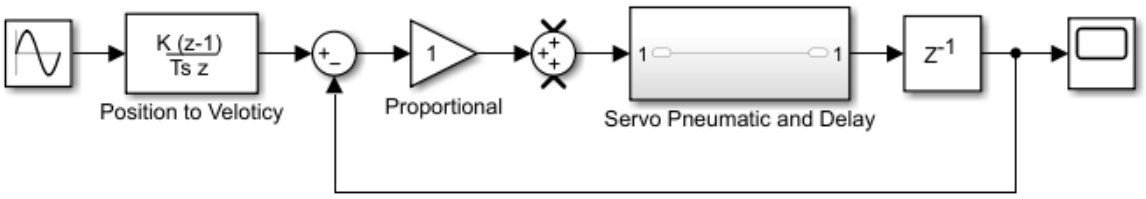

Figure 27. velocity proportional control for ankle angles (top) and a sine wave (middle) as well as the basic control diagram

This improvement is probably because valve actuator positions most directly correspond to velocity instead of position. Position control probably added an integrator to the system which magnified errors and overshoots, causing growing overshoot or instability. The large position bias is a hard tradeoff given that accuracy is part of project requirements, but the improved safety and consistency of this design is a net gain.

4.3.6 Variable Gain

All forms of the controller were difficult to tune and often needed changes for different tests or random variations in the supply pressure or friction. Loaded testing initially failed because the control gains need to be higher for the loaded direction of motion and the piston is asymmetrical. The controller was modified to slowly adjust the proportional gain based on position feedback independently for each direction of motion. This allows position bias correction to be re-introduced without instability. The gain modification is only locally stable and depends on the wall avoidance mode and upper and lower caps on gain adjustment to function indefinitely. Controller tests had to be run for six seconds for gain adjustment before data recording began to achieve consistent results.

4.3.7 Force Control

Force control is more often used with pneumatics in industry and PID based systems are commercially available. Development of force control for this prototype followed a similar pattern to position control. PID worked for a slow rate of change with a high damping (D) gain as shown in Figure 28, but it became marginally stable and then unstable as frequency or rate of change were increased. This design would also not work for human walking. Force control also has difficulty crossing zero, switching direction.

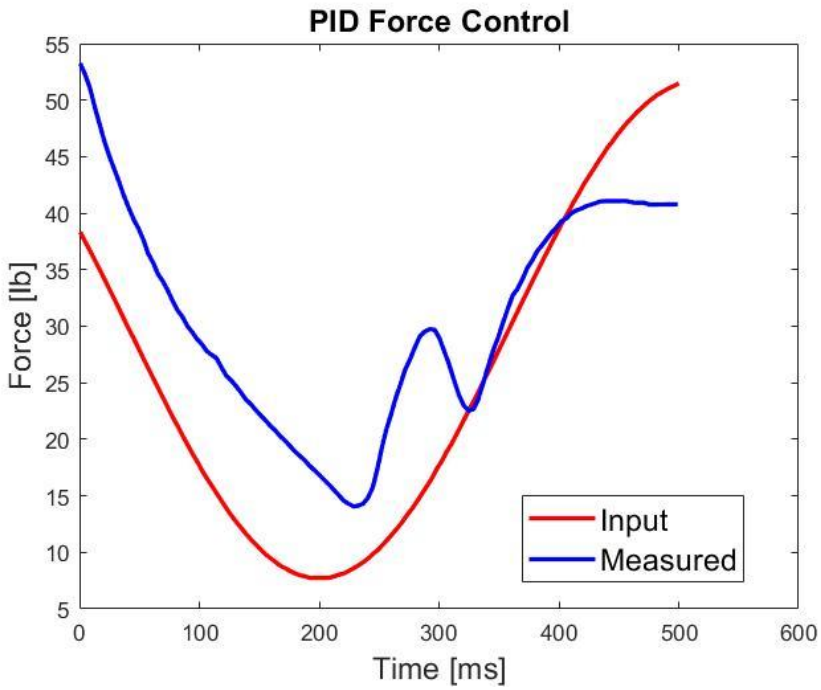

Figure 28. PID Force control for slow sine waves

4.3.8 Df/dt Control

Force control was improved in the same way as position control, by using the derivative of the input as the controller input. This is probably for the same reason as in position because opening valves corresponds to a change in force while a force can be

maintained by closing all valves. The derivative approach, shown in Figure 29; was able to follow the motion profile but with a positive bias. It also remained stable in all tests.

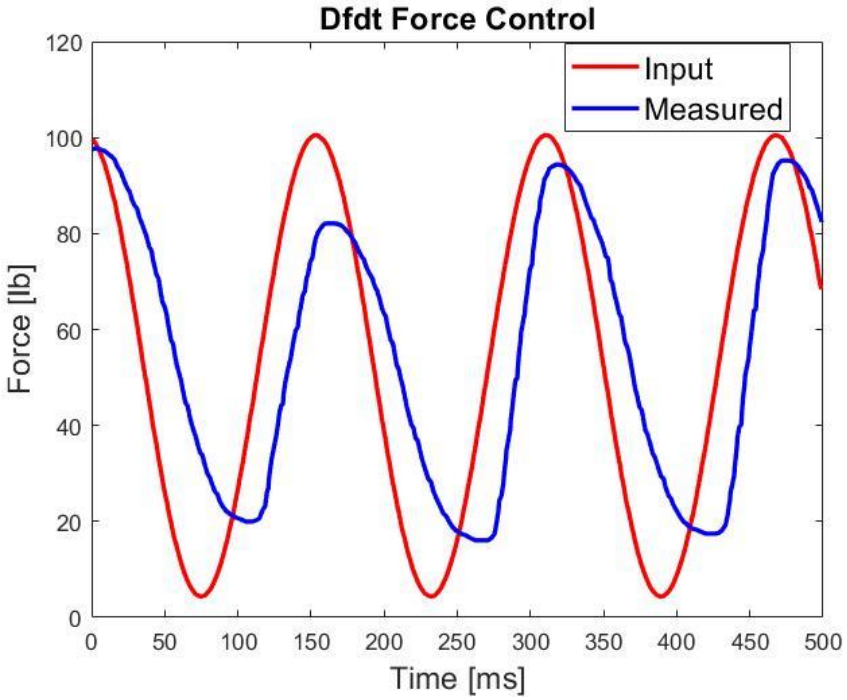

Figure 29. Force control testing, Dfdt method

4.3.9 Mode Switching

Derivative control did not solve the problem with switching direction or going to zero. A separate condition was added in which the actuator will fully open all valves when the desired force is zero or negative compared to the current force. Pressure drop in the cylinder when venting slows exponentially as it approaches zero. Near zero that drop becomes too slow so the controller was always biased to a higher than desired pressure. Zero mode minimized this problem although it still caused inaccuracy in walking trials.

4.4 Final Version Testing

4.4.1 Human Subject Testing

Pneumatic actuator testing used recorded ankle angle and moment data from eight subjects via motion capture (Vicon, Oxford, U.K.) and a ground-embedded force plate (AMTI, Waterford, MA, USA). Testing was performed on these eight subjects during level ground walking. All eight participants (4 males, 4 females, age 21.1 $\pm$1.7 years; height 171.5$\pm$11.6 cm; weight 150$\pm$30.5 lbs) provided written informed consent (Auburn University protocol approval No. 17-279-MR 1707). The subjects performed three walking trials each along a five-meter walkway with an average walking speed of 1.28 $\pm$ 0.12 m/s. One gait cycle per walking trial was analysed with Visual3D (C-Motion, Germantown, MD) for ankle kinematics. The side used, left or right, was randomly selected for each trial. Three repetitions of the same stride were recorded for each subject for each test and averaged together.

4.4.2 Final Position Control

The final position controller described mathematically in Equations (5) and (6) and in Figure 30, is a proportional velocity controller with overshoot compensation and a gain adjusted by position error. The controller derives the desired position to a velocity and measures error from the back EMF velocity sensor. Position error is taken from the potentiometer and the sent position is used to incrementally change the proportional gain for velocity control. The control gains have an upper limit to prevent dangerous overshoot if the air supply is shut off then restored. The overshoot compensator sums control inputs over 100ms and estimates the change in velocity in the next 100ms with no further input. Proportional control then references the measured velocity with this predicted change added to make further control inputs. There are also correction inputs

to limit jarring contacts with the cylinder endcaps by setting a velocity away from the endcap when the piston moves within 0.5 cm for each side. The controller is expected to closely follow the motion profile of the input and contain position bias. Equations (5) and (6) represent the control algorithm.

$$C = -\left(\frac{dx_d}{dt} - v_m\right) K_p - K_c \sum_{t-200}^{t} C \tag{5}$$

where

$$K_p = K_p - K_a(x_d - x_m) \tag{6}$$

For the algorithm, C is a control value, K_p is the proportional control gain which is adjusted every loop, K_a is a multiplier for adaptive gain, x is a position, v is velocity, d is desired measurement, and m is measured data. The adaptive control uses a separate K_p value for each direction of motion to account for uneven directional loading.

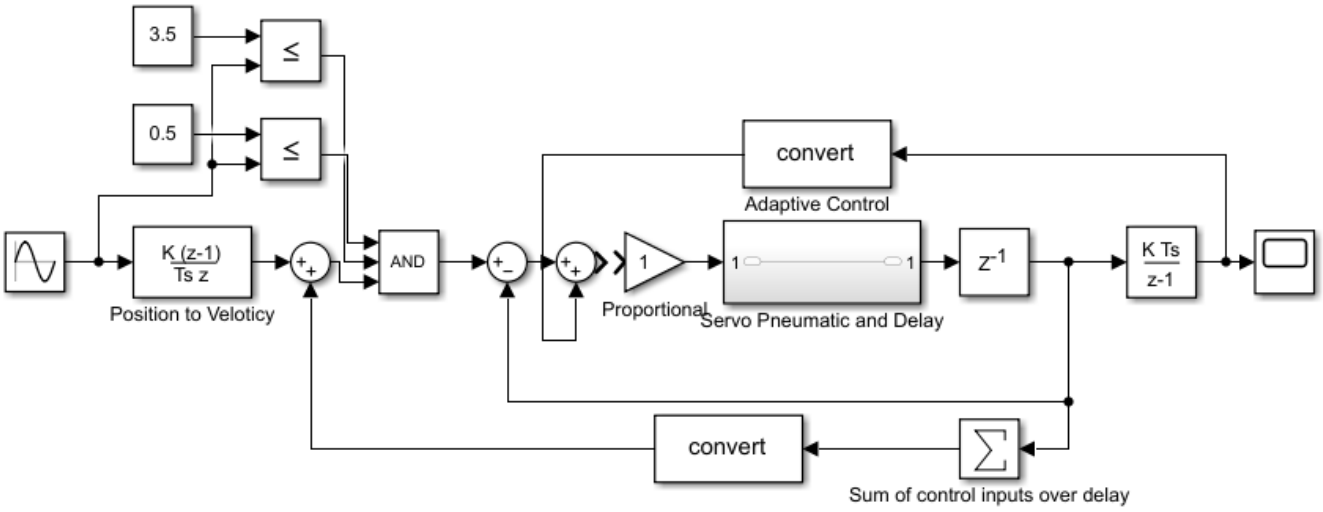

Figure 30. block diagram of the position controller

4.4.3 Stability Testing

First, the actuator tracked the position of sine waves at 1, 2, and 3 Hz to establish basic controller stability around the range of human walking with the position

controller active. The actuator was expected to track the wave at a constant amplitude with no additional oscillations introduced.

4.4.4 Position Testing

For the position control testing the actuator was sent ankle angles which were interpreted as linear positions with a 7 cm moment arm. The piston end was free and unloaded for its 10 cm range of motion.

For each of the four averaged trials the ankle kinematic data were converted to the corresponding linear actuator length based upon the exoskeleton design geometry and transmitted post hoc to the actuator controller in simulated real time. The step for each trial was repeated on a loop a minimum of four times so that the actuator could reach a steady operating state before recording. The measured position and force of the piston end were returned to the computer and recorded in real-time. For each trial RMSE was calculated between the input and measured data with delay offsets from zero to 400 ms at four ms increments. The minimum RMSE and its corresponding delay offset were recorded.

4.4.5 Final Force Control

Force control also uses a form of derivative control shown in Equations (5) and (6), from which the desired force is derived and compared to a measured change in force over time. It has the same effective block diagram as position control in Figure 30. The proportional gain is also adjusted based on the position error to compensate for loading. It has a similar overshoot compensator which adds the sum of control inputs over a 100 ms period to the measured position. The force control algorithm is represented in (7) and (8).

$$C = -\left(\frac{dF_d}{dt} - \frac{dF_m}{dt}\right) K_p \qquad (7)$$

where

$$K_p = K_p - K_a(F_d - F_m) \qquad (8)$$

In these equations F is for measured and desired force. Overshoot prediction did not improve results for this control method. All K values were initially set to manually tuned values.

4.4.6 Force Testing

Force control was first done with the piston end rigidly fixed to the cylinder body across an S type load cell, shown in Figure 31. On the second set of force test the rigid threaded rods were replaced with springs, shown in Figure 31 with a total spring constant of 107.2Ncm, to test the effect of applying force while extending. For both tests the actuator is given a series of ankle moments in real time which are converted to a linear force at a 7 cm moment arm. The force is divided by five to approximate a 20% assistance of biological plantarflexion during walking.

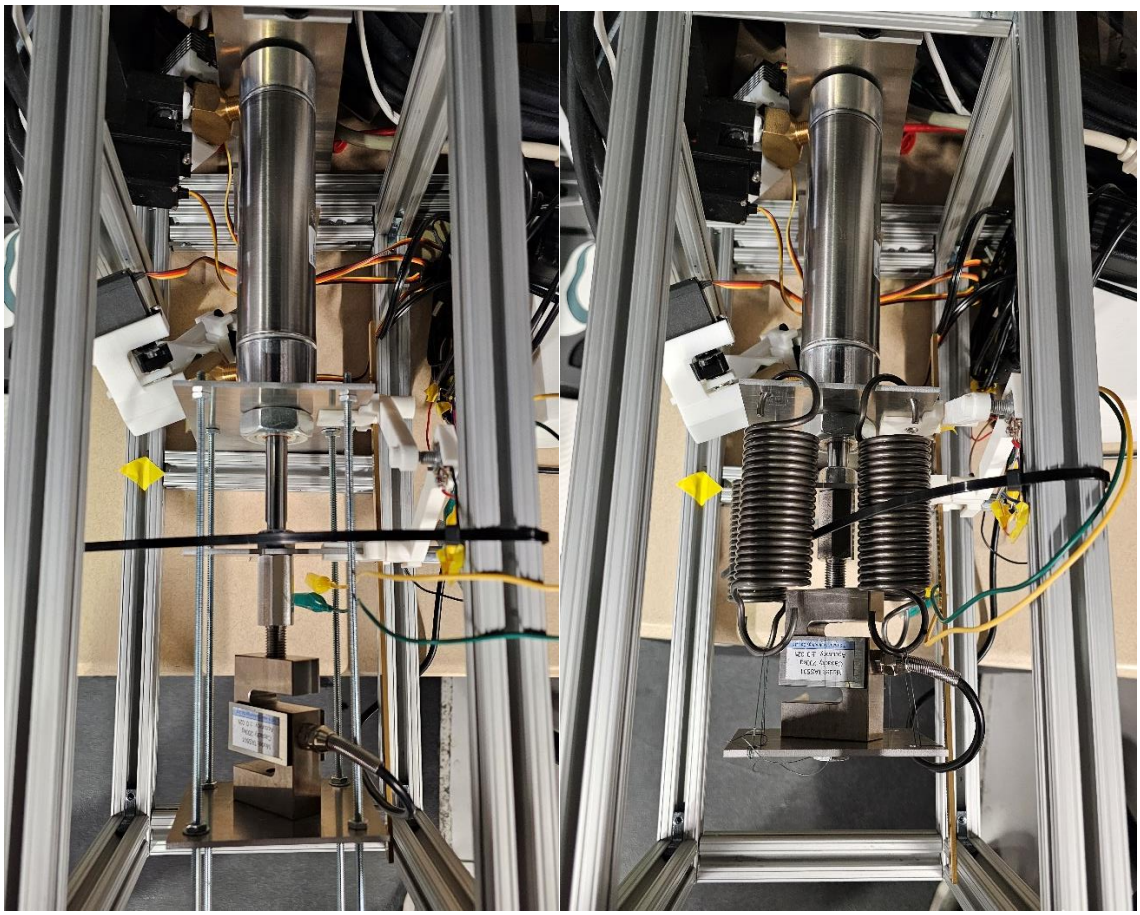
Figure 31; Force testing configuration with fixed rods (left) and springs (right)

4.5 Results

Figure 32 shows the result of stability testing with sine waves. Oscillations remain at the same frequency as the input wave and do not grow in amplitude. For the high frequency test, the amplitude falls below the input. These indicate that there is no positive feedback leading to instability.

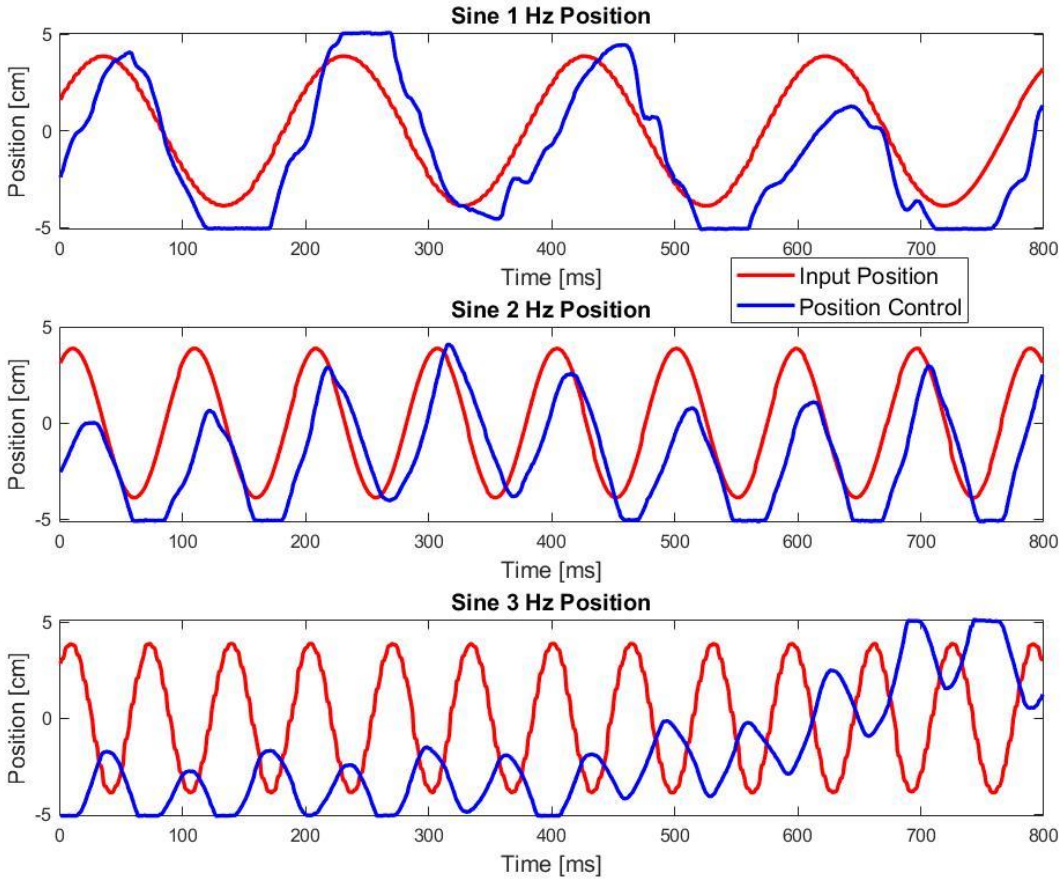

Figure 32. Stability testing with final controller version

Position control testing is shown in Figure 33. The motion profile is roughly followed but with a large position bias. Some unwanted oscillation is observed.

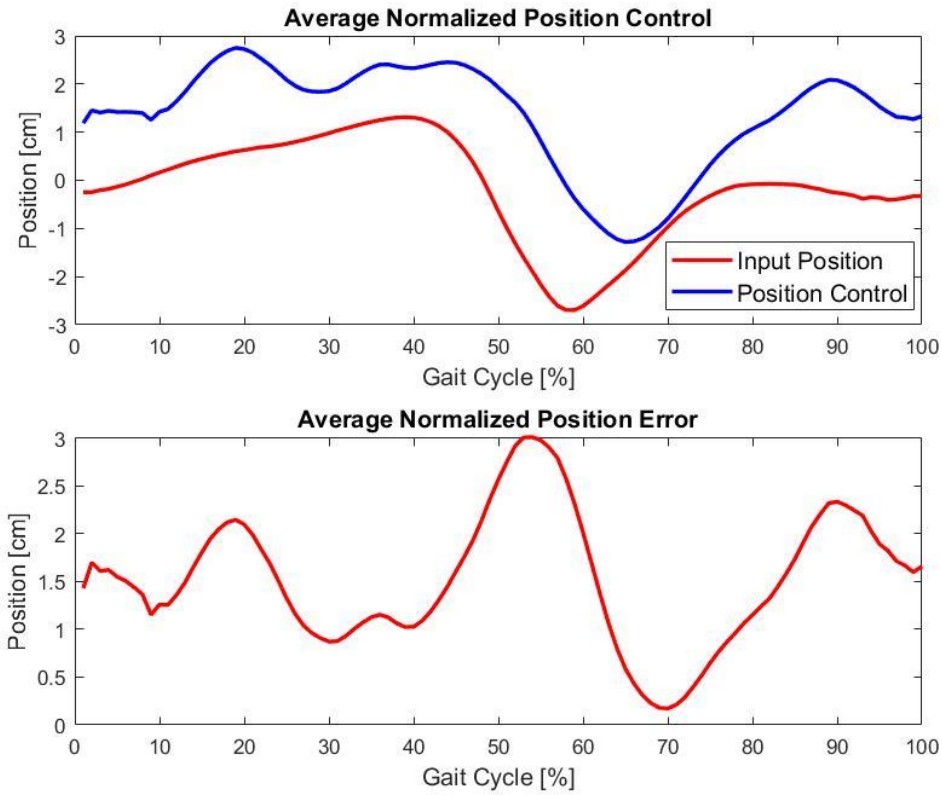

Figure 33. Position Control using ankle angle data

Force control is shown in Figure 34. The results show a large overshoot (~100%) and slow pressure release when zero force is commanded. The system provides a force but with far lower accuracy than the goal of 5% RMSE. It can only keep up with returning to zero between steps at a rate below the frequency of walking.

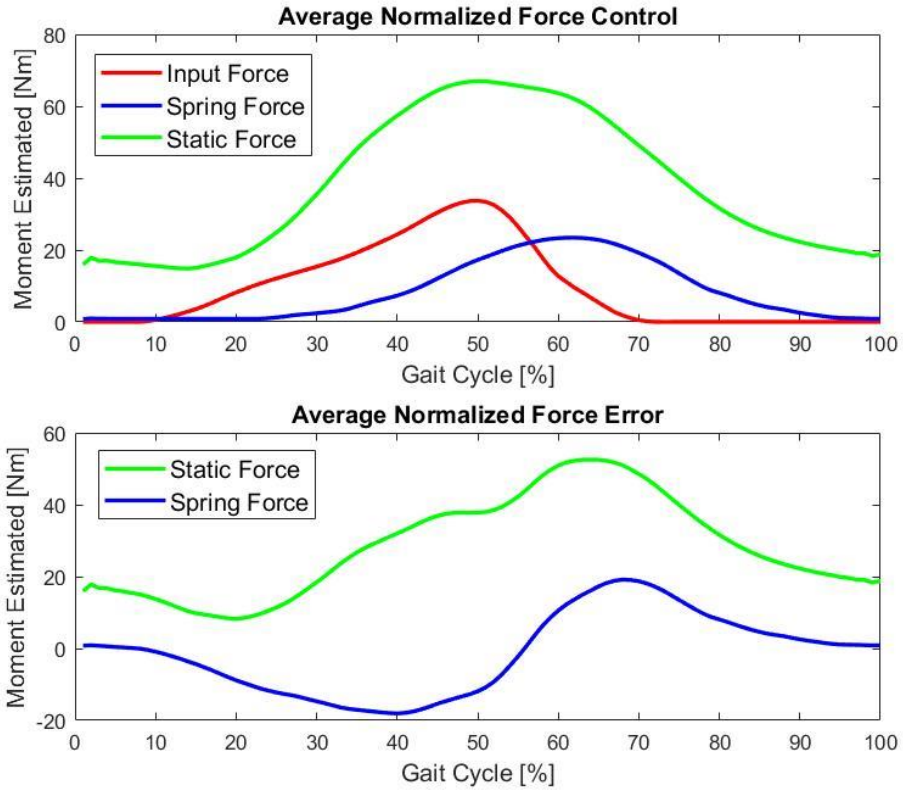

Figure 34. Force control using ankle moment data

Table 1 shows the RMSE values from testing and Table 2 shows delays as estimated control delays based on minimized RMSE. Delays were all within 50ms of 100ms. Velocity RMSE was also not within accuracy goals of 5% RMSE for the total range of motion for control.

Table 1, Pneumatic Control RMSE minimized

Controller	Position	Velocity	Static Force	Spring Force
RMSE avg. (cm)(Nm)	2.58	40.8	30.5	5.42
RMSE min (cm)(Nm)	1.09	36.1	26.26	2.39
RMSE max (cm)(Nm)	3.31	46.45	33.85	10.2

Table 2, Pneumatic Control Delays at minimum RMSE

Controller	Position	Velocity	Static Force	Spring Force

Delay avg. (ms)	70.82	96.35	123.96	168.75
Delay min (ms)	58.33	83.33	108.33	137.5
Delay max (ms)	104.16	116.66	133.33	195.8

4.7 Discussion

The goal of this study was to determine if a pneumatic actuator can meet requirements for force, speed, delay, and control to be used on an ankle exoskeleton. The actuator does not meet all of the requirements based on these tests. The actuator did meet the speed and force output specifications that it was designed for but lacked the control accuracy and response time to provide useful assistance to a wearer.

Estimated response delay was under 100ms for the unloaded position testing which does meet the requirement. However, during force control with load the delays reached over 200ms. Force control with high force output is a more realistic scenario for use to assist walking so this indicates a failure to meet the delay goal. Reaching a higher pressure for force generation is expected to take longer than for unloaded movement but the time difference was underestimated in the design process. During force control testing, the actuator failed to reduce force output at the rate the ankle moment reduces prior to toe off shown in Figure 34. In real use this would prevent dorsiflexion without a large external antagonistic force to assist. Based on testing of the system and servo motors most of the delay is from the time for pressure change to occur. The system adds about 10ms for communication and 30ms for the motor to begin to turn a valve. Airflow adds 40ms for unloaded conditions and over 100ms for loaded tests.

The stability requirement was met based on Figure 31. For the sine wave tests, amplitude and apparent delay remained within 10% of initial values for the test duration despite a moving position bias, indicating a stable system. While a mathematical simulation of the system plant was not accurate using normal gas flow equations, the controllers were never observed to produce a growing oscillation during testing, a step response, or while following sine waves at 1, 2 or 3 Hz. While there was no extreme instability there was a common oscillation in both controllers which severely reduced accuracy in all tests. The persistent oscillation also probably disrupted the adaptive gains and overshoot compensation for control causing them to have inconsistent effectiveness.

The accuracy target was not met for position or force control RMSE was far above 5% of the total range of motion. Velocity RMSE was also higher than the target velocity during position control probably due to the persistent oscillation in the system. The admittance control strategy was used because it is the most consistent and stable method for this cylinder, but it lacks direct position feedback which caused it to loosely follow the target position and hold a large bias. The position control bias also tended to wander above and below the average target position for several cycles at a time which is apparent in the 3 Hz sine wave test. This makes individual results highly inconsistent. This controller also had greater velocity and position accuracy on symmetrical, geometric patterns than on the irregular ankle angles. The equations for flow through an orifice appear to be inaccurate for the ball valves used and this in addition to the delays in the system caused control designs to become less stable than theoretically expected. The behavior of force control paralleled that of position control throughout development.

Control directly for force was unstable, sometimes oscillating between zero and maximum force, and could not be damped to a useable state however an admittance strategy using dF/dt lacked accuracy in exchange for stability.

The design of the pneumatic system involved problematic design tradeoffs and limitations. Larger diameter valves allow for faster airflow into or out of a cylinder but take longer to mechanically actuate which causes a large system delay. The piston for this actuator weighs about 500 g which forces the actuator to spend a high percentage of its capacity moving itself at the accelerations needed for ankle use which lowered efficiency and control compared to a low inertia Bowden cable or joint motor system. The high system delay, even with optimization, forces use of complex and less versatile control solutions. System delay was acceptable in the best-case scenario but increased quickly when the pressure differential was low or when the load requirement increased.

A pneumatic system inherently has a worse delay than a direct drive system because it has a two-stage response in which the valve actuator delay and pressure change response time stack. The final version of the valve assembly was well optimized for flow delay, but the servo valves were too slow to actuate to fully open and back to closed so the advantage of that design was never fully realized. The selected ball valves had a high torque requirement to turn so larger, slower geared servos were used. Solenoids may have improved the design despite flow restriction.

The system consumed compressed air equal to 33.5in^3 at one atmosphere per stroke under load which would exhaust a typical SCUBA tank in about 30 minutes using one cylinder for each leg. Pneumatic systems with a battery powered compressor are

only about 30% efficient for producing mechanical work compared to 90% for a direct motor drive [72].

The spring tests also indicate that force output is significantly reduced at high speed due to the limited volume flow rate of air through the valves. This may also be the root cause of the oscillation seen in position testing. When the piston moves forward under inertia, the air ahead of it is compressed while the air behind it expands. If the valves are not open far enough during fast movement the airflow does not keep up with the volume change the pressure difference can reverse and cause the piston to bounce backward without control input. This mechanic is why the overshoot compensation was not completely effective. It also caused the controller to overcompensate even more at random times which contributed to instability on position control designs.

4.8 Limitations

The study had limitations compared to a real exoskeleton use case. The actuator never provided a force load while moving in a realistic profile. Testing did not account for the response of a wearer to having the actuator assisting or impeding their motion and it did not account for the extra inertia of a foot and exoskeleton. The study also only used cyclic walking with identical steps which does not represent all possible motion while walking in a real environment. None of the test cases were able to perfectly replicate the motion and loads which would occur when being used on an ankle exoskeleton, especially with a wearer prediction model. A portable air supply or power source were also not considered for testing.

4.9 Conclusion

The actuator in its current form is not useable for an ankle exoskeleton. The system tested could not meet the accuracy or frequency requirements for useful walking assistance. It may have applications in low speed, high strength lifting applications due to the compliance and high force output. The position controller was able to remain stable in all conditions without a plant model which shows that accurate pneumatic cylinder assistance may be feasible with improved hardware.

Chapter 5

Future Work

There are potential strategies to improve the performance of the Maxon motor and minimize its limitations. Series elastic actuators have been shown to improve the compliance limitation of motors and this would be easy to implement on the spool or cable. A ball screw mechanism would reduce the weight and complexity of combining the safety stops, gearbox, and spool. Ball screws or lead screws are normally marketed for low-speed high force applications but there is no theoretical reason preventing their use for exoskeletons with a lower ratio gearbox on the motor. Other researchers have developed clutch or variable transmission mechanisms which overcome the top speed limitation of the motor by allowing the exoskeleton to either become passive or trade torque for speed [73]. It is also important to reduce the inertia of all moving parts because high accelerations are involved. The actuator can spend a high percentage of its power moving itself if mass is not low on the gearbox, spool, and boot.

An improved method of actuator performance evaluation is also needed. RMSE can verify if tracking is accurate and estimate average delay, but it does not offer any qualitative assessment of the type of inaccuracies involved such as overshoot, oscillation, speed or acceleration limitations, or variable delay. These causes of tracking

accuracy are important for selecting future design improvements and were only measured qualitatively in this study. Study of these measurements could also improve simulation of the actuators.

Given what was learned in the pneumatic actuator study it is possible to recommend an improved design to future researchers. The first change is to increase the operating pressure as much as possible and use proportionally smaller components. This allows for higher pressure differences within the system to improve response times, especially for returning to zero force output. Higher pressure allows for the use of smaller components such as the cylinder, valves, and servos. All of these contribute moving parts with inertia so reducing their size will improve the system response time even more. Smaller valves with low torque requirements will actuate faster than the ¼ inch models used here. This will also reduce the total weight of the actuator, making a more practical exoskeleton.

The pneumatic system should use a closed loop pressure cycle filled with Helium or Hydrogen instead of natural air. The rate of pressure change in the cylinder when a valve is opened at a given pressure differential is directly proportional to the speed of the individual gas molecules as they randomly bounce off of each other and the container. All gas molecules have the same kinetic energy at a given temperature so lighter molecules are moving faster. Air has a molecular weight of about 29 while Helium is 4 and Hydrogen is 2. Hydrogen leaks into the air can cause an explosion so Helium should be preferred for a wearable system. A system using these gases should have a pressure response about three times faster than an air filled system [74].

Combined with digital servos, this change could make a system competitive with large electric motors on time response.

Valves have less of a clear best answer, but the solution is probably to use a design with a short travel and solve the flow restriction problem with brute force in a higher-pressure system. Also, solenoids appear to have faster responses than servos, at least at small sizes so proportional solenoids are appear to be the best option with a higher pressure limit. Servo valves can also be optimized by reducing the travel distance and lowering torque so that faster geared servos can be used.

For controls, the proportional approach using the derivative inputs is the only method to ensure safety and stability, but other components of the controller need improvement. Other researchers familiar with machine learning believe that it could be used to predict overshoot and improve delay tolerance more accurately. The algorithm would be trained on control inputs, position, and velocity of the actuator during tests. It would then estimate the control delay and predict the effect of control inputs during that period, producing a corrected position measurement for the system. This technology may also be able to identify the system of the pneumatic for improved modeling or completely replace the controller with a reinforcement learning approach. Machine learning has been used to control pneumatic muscles in a similar way [75].

This work did not consider a portable power supply for the exoskeleton, but this is a concern in future research. Small battery powered compressors have been shown in research but are not powerful enough to meet the demand for walking in real time. A standard SCUBA tank could supply power for a pair of ankle exoskeletons walking for about 30 minutes according to rough calculations so pressure storage, while cheaper

than batteries, is not easy to make portable and possibly hazardous on the battlefield. Another speculative option is to use a chemical reaction in which storable liquid produces a gas at high pressure and reasonably low temperatures. Historically, metal acid reactions have been used in this way to fill balloons.

Pneumatic actuators may be better suited to other applications. Strength augmentation for logistics or construction is a better fit for the demonstrated capabilities. The high force to weight at a low cost, lower optimal movement speed, compliance to wearer movement could all contribute to safe and powerful strength amplification. Another route for pneumatic systems is to implement variable elasticity and damping in series with electric motors. This design has been demonstrated and could use a passive cylinder with actuated valves to store energy, adjust compliance with prediction certainty, or absorb shocks to the body to protect joints.

Chapter 6

Conclusion

This research was able to compare the capabilities and drawbacks of a novel actuation approach to a more standard design. Performance metrics were established to objectively evaluate the usefulness of an actuator for exoskeletons and tests were carried out to use them. The testing showed that each actuator has relative design tradeoffs making it useful for certain types of exoskeletons. The Maxon motor, representing motors used in recent research, has great controllability and efficiency. Its limitations are speed and compliance to the wearer. It is likely to waste energy pushing against the wearer without an extremely accurate prediction algorithm and low delay operation. It also raised safety concerns because of the unlimited range of motion.

A pneumatic system takes some of the burden away from perfectly predicting movement intent but replaces that challenge with controlling an unknown, nonlinear system. The pneumatic cylinder met the basic specifications, and stable but inaccurate control was demonstrated. It did demonstrate a high force to weight ratio, compliance to external forces during operation in the spring test, and much higher than needed movement speed. The electric motor appears to still be the superior option assuming a better microcontroller, but neither is practical for the goal of soldier augmentation

without excessive weight or battery changes. The pneumatic design could find a niche in future exoskeleton use where force output at low cost is the most important consideration.

Pneumatic control proved to be more difficult than expected based on theory. The high actuation speed relative to delay made stable position control effectively impossible. The velocity control method was counterintuitive and not ideal for positioning but did allow for safe movement at the intended speeds. It became difficult to apply normal control theory due to the lack of an accurate plant model or simulation. Adaptive gains were superior to iterative manual tuning but limited by prototype reliability.

This study raised several important concerns for any exoskeleton actuator design. Delay minimization is the most important concern because it directly impacts interaction with the wearer and discrete controller stability. Most off-the-shelf hardware and software, such as the Maxon controller used, is not delay optimized to the degree needed for this use. The pneumatic design suffered less from unnecessary delay by using analog sensors and servos and minimizing communication between devices. The controller, sensor readings, and servo commands all ran on a single microcontroller. Future actuators probably need to use custom embedded controllers for the best possible performance.

Actuator design also needs to consider mechanical safety from the beginning. Both actuators tested would be unable to pass IRB approval for human testing due to lack of safety stops and lack of damping respectively. Safety could be retrofitted, such

as with a safety stop mechanism on the ankle, but having this integrated early would reduce weight and complexity.

Actuation technology has not yet passed the capabilities of human muscle, at least without serious tradeoffs. True human augmentation will depend on further advances but the actuators tested could be useful in certain settings such as medical rehabilitation or industrial settings with external power. This study was able to expand lab knowledge of actuators, establish a process for evaluating them, and find areas for future exoskeleton research.

References

[1] K. Anam and A. A. Al-Jumaily, “Active Exoskeleton Control Systems: State of the Art,” *Procedia Engineering*, vol. 41, pp. 988–994, Jan. 2012, doi: 10.1016/j.proeng.2012.07.273.

[2] G. S. Sawicki and D. P. Ferris, “Mechanics and energetics of level walking with powered ankle exoskeletons,” *Journal of Experimental Biology*, vol. 211, no. 9, pp. 1402–1413, May 2008, doi: 10.1242/jeb.009241.

[3] H.-M. Wang, D. K. L. Le, and W.-C. Lin, “Evaluation of a Passive Upper-Limb Exoskeleton Applied to Assist Farming Activities in Fruit Orchards,” *Applied Sciences*, vol. 11, no. 2, Art. no. 2, Jan. 2021, doi: 10.3390/app11020757.

[4] R. Altenburger, D. Scherly, and K. S. Stadler, “Design of a passive, iso-elastic upper limb exoskeleton for gravity compensation,” *ROBOMECH Journal*, vol. 3, no. 1, p. 12, Apr. 2016, doi: 10.1186/s40648-016-0051-5.

[5] S. K. Banala, S. K. Agrawal, and J. P. Scholz, “Active Leg Exoskeleton (ALEX) for Gait Rehabilitation of Motor-Impaired Patients,” in *2007 IEEE 10th International Conference on Rehabilitation Robotics*, Jun. 2007, pp. 401–407. doi: 10.1109/ICORR.2007.4428456.

[6] J. Taborri *et al.*, “Sport Biomechanics Applications Using Inertial, Force, and EMG Sensors: A Literature Overview,” *Applied Bionics and Biomechanics*, vol. 2020, p. e2041549, Jun. 2020, doi: 10.1155/2020/2041549.

[7] A. Zoss, H. Kazerooni, and A. Chu, “On the mechanical design of the Berkeley Lower Extremity Exoskeleton (BLEEX),” in *2005 IEEE/RSJ International Conference on Intelligent Robots and Systems*, Aug. 2005, pp. 3465–3472. doi: 10.1109/IROS.2005.1545453.

[8] S. M. Siedl and M. Mara, “Exoskeleton acceptance and its relationship to self-efficacy enhancement, perceived usefulness, and physical relief: A field study among logistics workers,” *Wearable Technologies*, vol. 2, p. e10, Jan. 2021, doi: 10.1017/wtc.2021.10.

[9] S. Spada, L. Ghibaudo, S. Gilotta, L. Gastaldi, and M. P. Cavatorta, “Investigation into the Applicability of a Passive Upper-limb Exoskeleton in Automotive Industry,” *Procedia Manufacturing*, vol. 11, pp. 1255–1262, Jan. 2017, doi: 10.1016/j.promfg.2017.07.252.

[10] P. Malcolm, W. Derave, S. Galle, and D. D. Clercq, “A Simple Exoskeleton That Assists Plantarflexion Can Reduce the Metabolic Cost of Human Walking,” *PLOS ONE*, vol. 8, no. 2, p. e56137, Feb. 2013, doi: 10.1371/journal.pone.0056137.

[11] M. Goršič, Y. Song, B. Dai, and D. Novak, “Evaluation of the HeroWear Apex back-assist exosuit during multiple brief tasks,” *Journal of Biomechanics*, vol. 126, p. 110620, Sep. 2021, doi: 10.1016/j.jbiomech.2021.110620.

[12] B. Kim and A. D. Deshpande, “An upper-body rehabilitation exoskeleton Harmony with an anatomical shoulder mechanism: Design, modeling, control, and performance evaluation,” *The International Journal of Robotics Research*, vol. 36, no. 4, pp. 414–435, Apr. 2017, doi: 10.1177/0278364917706743.

[13] R. Goergen, A. C. Valdiero, L. A. Rasia, M. Oberdörfer, J. P. de Souza, and R. S. Gonçalves, “Development of a Pneumatic Exoskeleton Robot for Lower Limb

Rehabilitation," in *2019 IEEE 16th International Conference on Rehabilitation Robotics (ICORR)*, Jun. 2019, pp. 187–192. doi: 10.1109/ICORR.2019.8779522.
[14] L. R. Bunge *et al.*, "Effectiveness of powered exoskeleton use on gait in individuals with cerebral palsy: A systematic review," *PLOS ONE*, vol. 16, no. 5, p. e0252193, May 2021, doi: 10.1371/journal.pone.0252193.
[15] S. Wang *et al.*, "Design and Control of the MINDWALKER Exoskeleton," *IEEE Transactions on Neural Systems and Rehabilitation Engineering*, vol. 23, no. 2, pp. 277–286, Mar. 2015, doi: 10.1109/TNSRE.2014.2365697.
[16] P. Yin, L. Yang, S. Qu, and C. Wang, "Effects of a passive upper extremity exoskeleton for overhead tasks," *Journal of Electromyography and Kinesiology*, vol. 55, p. 102478, Dec. 2020, doi: 10.1016/j.jelekin.2020.102478.
[17] S. Iranzo, A. Piedrabuena, D. Iordanov, U. Martinez-Iranzo, and J.-M. Belda-Lois, "Ergonomics assessment of passive upper-limb exoskeletons in an automotive assembly plant," *Applied Ergonomics*, vol. 87, p. 103120, Sep. 2020, doi: 10.1016/j.apergo.2020.103120.
[18] H. K. Yap, J. H. Lim, F. Nasrallah, J. C. H. Goh, and R. C. H. Yeow, "A soft exoskeleton for hand assistive and rehabilitation application using pneumatic actuators with variable stiffness," in *2015 IEEE International Conference on Robotics and Automation (ICRA)*, May 2015, pp. 4967–4972. doi: 10.1109/ICRA.2015.7139889.
[19] A. S. Koopman *et al.*, "Biomechanical evaluation of a new passive back support exoskeleton," *Journal of Biomechanics*, vol. 105, p. 109795, May 2020, doi: 10.1016/j.jbiomech.2020.109795.
[20] S. Song and S. H. Collins, "Optimizing Exoskeleton Assistance for Faster Self-Selected Walking," *IEEE Transactions on Neural Systems and Rehabilitation Engineering*, vol. 29, pp. 786–795, 2021, doi: 10.1109/TNSRE.2021.3074154.
[21] T. Luger, R. Seibt, T. J. Cobb, M. A. Rieger, and B. Steinhilber, "Influence of a passive lower-limb exoskeleton during simulated industrial work tasks on physical load, upper body posture, postural control and discomfort," *Applied Ergonomics*, vol. 80, pp. 152–160, Oct. 2019, doi: 10.1016/j.apergo.2019.05.018.
[22] J.-F. Zhang, C.-J. Yang, Y. Chen, Y. Zhang, and Y.-M. Dong, "Modeling and control of a curved pneumatic muscle actuator for wearable elbow exoskeleton," *Mechatronics*, vol. 18, no. 8, pp. 448–457, Oct. 2008, doi: 10.1016/j.mechatronics.2008.02.006.
[23] D. G. Caldwell, G. A. Medrano-Cerda, and M. Goodwin, "Control of pneumatic muscle actuators," *IEEE Control Systems Magazine*, vol. 15, no. 1, pp. 40–48, Feb. 1995, doi: 10.1109/37.341863.
[24] J. L. A. S. Ramos and M. A. Meggiolaro, "Use of surface electromyography for human amplification using an exoskeleton driven by artificial pneumatic muscles," in *5th IEEE RAS/EMBS International Conference on Biomedical Robotics and Biomechatronics*, Aug. 2014, pp. 585–590. doi: 10.1109/BIOROB.2014.6913841.
[25] H. Aschemann and D. Schindele, "Sliding-Mode Control of a High-Speed Linear Axis Driven by Pneumatic Muscle Actuators," *IEEE Transactions on Industrial Electronics*, vol. 55, no. 11, pp. 3855–3864, Nov. 2008, doi: 10.1109/TIE.2008.2003202.

[26] J. Lynch-Michigan, “Users control this ankle exoskeleton,” Futurity. Accessed: Nov. 27, 2023. [Online]. Available: https://www.futurity.org/ankle-exoskeleton-2719862/
[27] Y. Mitsutake, K. Hirata, and Y. Ishihara, “Dynamic response analysis of a linear solenoid actuator,” *IEEE Transactions on Magnetics*, vol. 33, no. 2, pp. 1634–1637, Mar. 1997, doi: 10.1109/20.582582.
[28] M. Schier and A. Lelkes, *Low-Noise EC Motor with External Rotor for Automotive Application*. 2002.
[29] J. Zhang *et al.*, “Human-in-the-loop optimization of exoskeleton assistance during walking,” *Science*, vol. 356, no. 6344, pp. 1280–1284, Jun. 2017, doi: 10.1126/science.aal5054.
[30] J. F. Veneman, R. Ekkelenkamp, R. Kruidhof, F. C. T. van der Helm, and H. van der Kooij, “Design of a series elastic- and Bowden cable-based actuation system for use as torque-actuator in exoskeleton-type training,” in *9th International Conference on Rehabilitation Robotics, 2005. ICORR 2005.*, Jun. 2005, pp. 496–499. doi: 10.1109/ICORR.2005.1501150.
[31] C. Meijneke, W. van Dijk, and H. van der Kooij, “Achilles: An autonomous lightweight ankle exoskeleton to provide push-off power,” in *5th IEEE RAS/EMBS International Conference on Biomedical Robotics and Biomechatronics*, Aug. 2014, pp. 918–923. doi: 10.1109/BIOROB.2014.6913898.
[32] N. Paine, S. Oh, and L. Sentis, “Design and Control Considerations for High-Performance Series Elastic Actuators,” *IEEE/ASME Transactions on Mechatronics*, vol. 19, no. 3, pp. 1080–1091, Jun. 2014, doi: 10.1109/TMECH.2013.2270435.
[33] H. Zheng, M. Wu, and X. Shen, “Pneumatic Variable Series Elastic Actuator,” *Journal of Dynamic Systems, Measurement, and Control*, vol. 138, no. 8, Jun. 2016, doi: 10.1115/1.4033620.
[34] D. Copaci, E. Cano, L. Moreno, and D. Blanco, “New Design of a Soft Robotics Wearable Elbow Exoskeleton Based on Shape Memory Alloy Wire Actuators,” *Applied Bionics and Biomechanics*, vol. 2017, p. e1605101, Sep. 2017, doi: 10.1155/2017/1605101.
[35] H. I. Ali, S. Bahari, M. Noor, S. M. Bashi, and M. H. Marhaban, “A review of pneumatic actuators (modeling and control.”
[36] B. M. Otten, R. Weidner, and A. Argubi-Wollesen, “Evaluation of a Novel Active Exoskeleton for Tasks at or Above Head Level,” *IEEE Robotics and Automation Letters*, vol. 3, no. 3, pp. 2408–2415, Jul. 2018, doi: 10.1109/LRA.2018.2812905.
[37] J. E. Pratt, B. T. Krupp, C. J. Morse, and S. H. Collins, “The RoboKnee: an exoskeleton for enhancing strength and endurance during walking,” in *IEEE International Conference on Robotics and Automation, 2004. Proceedings. ICRA ’04. 2004*, Apr. 2004, pp. 2430-2435 Vol.3. doi: 10.1109/ROBOT.2004.1307425.
[38] U. Heo, S. J. Kim, and J. Kim, “Backdrivable and Fully-Portable Pneumatic Back Support Exoskeleton for Lifting Assistance,” *IEEE Robotics and Automation Letters*, vol. 5, no. 2, pp. 2047–2053, Apr. 2020, doi: 10.1109/LRA.2020.2969169.
[39] T. Iwawaki, T. Noritsugu, D. Sasaki, and M. Takaiwa, “DEVELOPMENT OF PORTABLE ENERGY-SAVING TYPE AIR SUPPLY SYSTEM USING VARIABLE VOLUME TANK,” 2011.

[40] A. Haselbacher, F. Najjar, S. Balachandar, and Y. Ling, “Lagrangian Simulations of Shock-Wave Diffraction at a Right-Angled Corner in a Particle-Laden Gas,” vol. 60, p. AT.004, Nov. 2007.
[41] E. E. Topçu, İ. Yüksel, and Z. Kamış, “Development of electro-pneumatic fast switching valve and investigation of its characteristics,” *Mechatronics*, vol. 16, no. 6, pp. 365–378, Jul. 2006, doi: 10.1016/j.mechatronics.2006.01.005.
[42] N. D. Vaughan and J. B. Gamble, “The Modeling and Simulation of a Proportional Solenoid Valve,” *Journal of Dynamic Systems, Measurement, and Control*, vol. 118, no. 1, pp. 120–125, Mar. 1996, doi: 10.1115/1.2801131.
[43] B. Hejrati and F. Najafi, “Accurate pressure control of a pneumatic actuator with a novel pulse width modulation–sliding mode controller using a fast switching On/Off valve,” *Proceedings of the Institution of Mechanical Engineers, Part I: Journal of Systems and Control Engineering*, vol. 227, no. 2, pp. 230–242, Feb. 2013, doi: 10.1177/0959651812459303.
[44] L. Gao, C. Wu, D. Zhang, X. Fu, and B. Li, “Research on a high-accuracy and high-pressure pneumatic servo valve with aerostatic bearing for precision control systems,” *Precision Engineering*, vol. 60, pp. 355–367, Nov. 2019, doi: 10.1016/j.precisioneng.2019.09.005.
[45] L. C. Benson, N. U. Ahamed, D. Kobsar, and R. Ferber, “New considerations for collecting biomechanical data using wearable sensors: Number of level runs to define a stable running pattern with a single IMU,” *Journal of Biomechanics*, vol. 85, pp. 187–192, Mar. 2019, doi: 10.1016/j.jbiomech.2019.01.004.
[46] A. Pfister, A. M. West, S. Bronner, and J. A. Noah, “Comparative abilities of Microsoft Kinect and Vicon 3D motion capture for gait analysis,” *Journal of Medical Engineering & Technology*, vol. 38, no. 5, pp. 274–280, Jul. 2014, doi: 10.3109/03091902.2014.909540.
[47] Y. Sun, Y. Tang, J. Zheng, D. Dong, X. Chen, and L. Bai, “From sensing to control of lower limb exoskeleton: a systematic review,” *Annual Reviews in Control*, vol. 53, pp. 83–96, Jan. 2022, doi: 10.1016/j.arcontrol.2022.04.003.
[48] G. Aguirre-Ollinger, J. E. Colgate, M. A. Peshkin, and A. Goswami, “Active-Impedance Control of a Lower-Limb Assistive Exoskeleton,” in *2007 IEEE 10th International Conference on Rehabilitation Robotics*, Jun. 2007, pp. 188–195. doi: 10.1109/ICORR.2007.4428426.
[49] K. E. Gordon and D. P. Ferris, “Learning to walk with a robotic ankle exoskeleton,” *Journal of Biomechanics*, vol. 40, no. 12, pp. 2636–2644, Jan. 2007, doi: 10.1016/j.jbiomech.2006.12.006.
[50] J. A. George *et al.*, “Robust Torque Predictions From Electromyography Across Multiple Levels of Active Exoskeleton Assistance Despite Non-linear Reorganization of Locomotor Output,” *Frontiers in Neurorobotics*, vol. 15, 2021, Accessed: Sep. 21, 2023. [Online]. Available: https://www.frontiersin.org/articles/10.3389/fnbot.2021.700823
[51] M. S. AL-Quraishi, I. Elamvazuthi, S. A. Daud, S. Parasuraman, and A. Borboni, “EEG-Based Control for Upper and Lower Limb Exoskeletons and Prostheses: A Systematic Review,” *Sensors*, vol. 18, no. 10, Art. no. 10, Oct. 2018, doi: 10.3390/s18103342.

[52] S. Gonzalez, P. Stegall, S. M. Cain, H. C. Siu, and L. Stirling, “Assessment of a powered ankle exoskeleton on human stability and balance,” *Applied Ergonomics*, vol. 103, p. 103768, Sep. 2022, doi: 10.1016/j.apergo.2022.103768.
[53] M. K. Shepherd, D. D. Molinaro, G. S. Sawicki, and A. J. Young, “Deep Learning Enables Exoboot Control to Augment Variable-Speed Walking,” *IEEE Robotics and Automation Letters*, vol. 7, no. 2, pp. 3571–3577, Apr. 2022, doi: 10.1109/LRA.2022.3147565.
[54] R. P. Borase, D. K. Maghade, S. Y. Sondkar, and S. N. Pawar, “A review of PID control, tuning methods and applications,” *Int. J. Dynam. Control*, vol. 9, no. 2, pp. 818–827, Jun. 2021, doi: 10.1007/s40435-020-00665-4.
[55] D. Saravanakumar, B. Mohan, and T. Muthuramalingam, “A review on recent research trends in servo pneumatic positioning systems,” *Precision Engineering*, vol. 49, pp. 481–492, Jul. 2017, doi: 10.1016/j.precisioneng.2017.01.014.
[56] *Position Control with Rod Lock Cylinder - Enfield Technologies*, (Feb. 11, 2014). Accessed: Nov. 27, 2023. [Online Video]. Available: https://www.youtube.com/watch?app=desktop&v=SWpyqvrr-fU
[57] E. Franco and M. Ristic, “Time delay controller for the position control of a MRI-compatible pneumatic actuation with long supply lines,” in *2014 IEEE/ASME International Conference on Advanced Intelligent Mechatronics*, Jul. 2014, pp. 683–689. doi: 10.1109/AIM.2014.6878158.
[58] J. Wang, J. Pu, and P. Moore, “A practical control strategy for servo-pneumatic actuator systems,” *Control Engineering Practice*, vol. 7, no. 12, pp. 1483–1488, Dec. 1999, doi: 10.1016/S0967-0661(99)00115-X.
[59] G. Belforte, S. Mauro, and G. Mattiazzo, “A method for increasing the dynamic performance of pneumatic servosystems with digital valves,” *Mechatronics*, vol. 14, no. 10, pp. 1105–1120, Dec. 2004, doi: 10.1016/j.mechatronics.2004.06.006.
[60] O. A. Gaheen, E. Benini, M. A. Khalifa, and M. A. Aziz, “Pneumatic cylinder speed and force control using controlled pulsating flow,” *Engineering Science and Technology, an International Journal*, vol. 35, p. 101213, Nov. 2022, doi: 10.1016/j.jestch.2022.101213.
[61] M. Parnichkun and C. Ngaecharoenkul, “Kinematics control of a pneumatic system by hybrid fuzzy PID,” *Mechatronics*, vol. 11, no. 8, pp. 1001–1023, Dec. 2001, doi: 10.1016/S0957-4158(00)00040-4.
[62] T. Nuchkrua and T. Leephakpreeda, “Fuzzy Self-Tuning PID Control of Hydrogen-Driven Pneumatic Artificial Muscle Actuator,” *J Bionic Eng*, vol. 10, no. 3, pp. 329–340, Sep. 2013, doi: 10.1016/S1672-6529(13)60228-0.
[63] X. B. Tran, V. L. Nguyen, and K. D. Tran, “Effects of friction models on simulation of pneumatic cylinder,” *Mechanical Sciences*, vol. 10, no. 2, pp. 517–528, Oct. 2019, doi: 10.5194/ms-10-517-2019.
[64] G. M. Bone and S. Ning, “Experimental Comparison of Position Tracking Control Algorithms for Pneumatic Cylinder Actuators,” *IEEE/ASME Transactions on Mechatronics*, vol. 12, no. 5, pp. 557–561, Oct. 2007, doi: 10.1109/TMECH.2007.905718.
[65] H. Kazerooni, “Pneumatic force control for robotic systems,” in *Proceedings of the IEEE International Conference on Mechatronics, 2004. ICM ’04.*, Jun. 2004, pp. 231–236. doi: 10.1109/ICMECH.2004.1364443.

[66] J. F. Carneiro and F. G. de Almeida, “Using two servovalves to improve pneumatic force control in industrial cylinders,” *Int J Adv Manuf Technol*, vol. 66, no. 1, pp. 283–301, Apr. 2013, doi: 10.1007/s00170-012-4324-8.
[67] C. Ying, Z. Jia-fan, Y. Can-jun, and N. Bin, “Design and hybrid control of the pneumatic force-feedback systems for Arm-Exoskeleton by using on/off valve,” *Mechatronics*, vol. 17, no. 6, pp. 325–335, Jul. 2007, doi: 10.1016/j.mechatronics.2007.04.001.
[68] B. F. Mentiplay, M. Banky, R. A. Clark, M. B. Kahn, and G. Williams, “Lower limb angular velocity during walking at various speeds,” *Gait & Posture*, vol. 65, pp. 190–196, Sep. 2018, doi: 10.1016/j.gaitpost.2018.06.162.
[69] Ş. U. Yavuz, A. Şendemir-Ürkmez, and K. S. Türker, “Effect of gender, age, fatigue and contraction level on electromechanical delay,” *Clinical Neurophysiology*, vol. 121, no. 10, pp. 1700–1706, Oct. 2010, doi: 10.1016/j.clinph.2009.10.039.
[70] “Online shop for high precise drive systems by maxon | maxon group.” Accessed: Oct. 02, 2023. [Online]. Available: https://www.maxongroup.com/maxon/view/category/motor?etcc_cu=onsite&etcc_med_onsite=Product&etcc_cmp_onsite=EC-4pole+Program&etcc_plc=Overview-Page-Brushless-DC-Motors&etcc_var=%5bcom%5d%23en%23_d_&target=filter&filterCategory=ec4pole
[71] A. H. Hansen, D. S. Childress, S. C. Miff, S. A. Gard, and K. P. Mesplay, “The human ankle during walking: implications for design of biomimetic ankle prostheses,” *Journal of Biomechanics*, vol. 37, no. 10, pp. 1467–1474, Oct. 2004, doi: 10.1016/j.jbiomech.2004.01.017.
[72] V. Blagojevic, D. Seslija, S. Dudic, and S. Randjelovic, “Energy Efficiency of Pneumatic Cylinder Control with Different Levels of Compressed Air Pressure and Clamping Cartridge,” *Energies*, vol. 13, no. 14, Art. no. 14, Jan. 2020, doi: 10.3390/en13143711.
[73] G. Elliott, A. Marecki, and H. Herr, “Design of a Clutch–Spring Knee Exoskeleton for Running,” *Journal of Medical Devices*, vol. 8, no. 3, p. 031002, Sep. 2014, doi: 10.1115/1.4027841.
[74] S. Thunborg, G. E. Ingram, and R. A. Graham, “Compressed Gas Gun for Controlled Planar Impacts Over a Wide Velocity Range,” *Review of Scientific Instruments*, vol. 35, no. 1, pp. 11–14, Jan. 1964, doi: 10.1063/1.1718685.
[75] Y. Cao and J. Huang, “Neural-network-based nonlinear model predictive tracking control of a pneumatic muscle actuator-driven exoskeleton,” *IEEE/CAA Journal of Automatica Sinica*, vol. 7, no. 6, pp. 1478–1488, Nov. 2020, doi: 10.1109/JAS.2020.1003351.